Márcio Martins

Long term carbon storage in seagrass meadows and saltmarshes in the Ria Formosa along a hydrodynamic gradient

University of the Algarve

Faculty of sciences and technologies

2017

Márcio Martins

Long term carbon storage in seagrass meadows and saltmarshes in the Ria Formosa along a hydrodynamic gradient

Masters in Marine Biology

Work performed under the orientation of:

Prof. Rui Santos

Prof. Cristina Veiga Pires

University of the Algarve

Faculty of sciences and technologies

2017

Long term carbon storage in seagrass meadows and saltmarshes in the Ria Formosa along a hydrodynamic gradient

Declaration of Authorship

I declare to be the author of this work, which is original and unprecedented. Authors and works that were consulted are properly cited in text and are part of the reference list included.

_____

(Márcio Martins)

Acknowledgements

As per usual in this kind of work, help from many people was crucial. I'd like to thank the entirety of the ALGAE group, for giving me the opportunity of being part of the RIAVALUE project, as well as trusting me to carry on such a large (and sometimes expensive) part of the work.

To my advisor (Rui Santos) and co-advisor (Cristina V. Pires), I appreciate the time spent to share your expertise with me, helping me plan the best way to perform sampling and lab work, providing me access to the necessary equipment, analyze and report the data obtained from it. In this role I would also like to thank Carmen B. Santos, for her help with my R scripts for the analysis, statistical testing and guidance on how to improve my writing style. Your many hours spent reviewing and commenting my manuscripts were immensely appreciated.

The people who made the sampling process possible must also be thanked: André Silva and Cátia Freitas, thank you for helping me all throughout the very long days of the sampling campaigns that sometimes required us to get ready to work as the sun rose and leave after it had set. To Paulo Santana for his help explaining the practical aspects of core sampling and granulometric analysis, as well as providing access the necessary equipment.

Finally, as usual, no one lives from work alone. To the network of friends and family that were with me throughout all this time, even if from a large distance, I want to thank for all your support.

Abstract

Identification, quantification and monetization of ecosystem services is key for current ecosystem management and policy making. Current estimates of global organic carbon stocks in seagrass meadows and saltmarshes suffer from overrepresentation of certain species and do not account for variation in carbon storage due to abiotic factors. Sediment cores were extracted in *Zostera noltei* and *Spartina maritima* habitats along a hydrodynamic gradient in the Ria Formosa, a location that was converted to a clam farm and an area colonized by *Caulerpa prolifera*. Vegetation at those locations was also described. Organic carbon storage, contribution of the main organic matter sources to the sediment and vegetation properties were analyzed. Relations to estimate organic carbon and total nitrogen using organic matter values were estimated and the possibility of using sediment color to estimate organic matter was investigated. *Z. noltei* and *S. maritima* both stored similar amounts of carbon, on average 2.2 times more than the clam farm. The effect of hydrodynamics was significant, with carbon storage capacities in *Z. noltei* and *S. maritima* increasing by a maximum factor of 2.08 and 3.44 (respectively), from the most exposed to most sheltered station. Suspended particulate organic matter and autochthonous organic matter were the major contributors to sedimentary organic matter, with a bigger contribution from the former in *Z. noltei* sediment. No significant differences in contributions were found along the hydrodynamic gradient. Organic carbon storage in *Z. noltei* and *S. maritima* fell below reported global means, with the difference becoming even more drastic in high hydrodynamics areas. Understanding carbon storage variation and increasing the diversity of conditions under which they are measured is a key point to increase accuracy of carbon stocks estimations both at a global and local scale.

Keywords: ecosystem services; organic carbon stocks; saltmarshes; saltmarshes; Ria Formosa.

.

Resumo

Os serviços ecossistémicos providenciam vários benefícios à população humana. Alguns destes são úteis para o nosso bem-estar, enquanto que outros são absolutamente essenciais às populações nas áreas que estes abrangem. Atualmente, o sistema que se tem mostrado mais eficaz para a sua gestão consiste na sua monetização e entrada no mercado. Este sistema permite uma formulação e adoção de políticas ambientais baseada em valores quantitativos, através de uma análise custo-benefício entre o aumento do rigor da proteção aplicada a um ecossistema e um aumento da sua exploração. Este tipo de análise tem revelado que, por vezes, a substituição de um serviço ecossistémico tem um custo superior ao benefício económico trazido por uma atividade que o prejudicaria. A desvantagem deste sistema é a necessidade de identificar, quantificar e monetizar corretamente estes serviços, sob o risco de subestimação da importância do ecossistema. O sequestro de carbono atmosférico é um dos serviços ecossistémicos prestados por áreas costeiras vegetadas, tal como pradarias de ervas marinhas e sapais. Este carbono está incluído no chamado Carbono Azul, carbono sequestrado em áreas oceânicas. Apesar de constituírem uma pequena percentagem da área marítima, as áreas vegetais costeiras representam mais de metade dos stocks de carbono azul. O aumento da pressão internacional nos governos para gerirem as suas emissões de dióxido de carbono tem levado a um forte interesse em estimar a capacidade destes habitats em sequestrar carbono, de modo a permitir uma eficaz avaliação e monetização.

Cores de sedimento foram retirados em 10 estações na Ria Formosa, Portugal. Estes foram retirados em 4 habitats diferentes: pradarias de *Zostera noltei*, sapais de *Spartina maritima*, uma zona de viveiro de amêijoas e uma zona colonizada por *Caulera prolifera*. Nos habitats de *Z. noltei* e *S. maritima*, quatro cores foram retirados ao longo de um gradiente hidrodinâmico. Estes cores foram analisados ao longo da sua profundidade, sendo efetuada uma descrição do perfil sedimentar e medições da cor do sedimento. Subamostras foram feitas a cada 2 cm e para análises do conteúdo de matéria orgânica, carbono orgânico, azoto total, $\delta^{13}C_{org}$, $\delta^{15}N_{total}$. O conteúdo de carbono orgânico foi combinado com medições de densidade aparente seca para estimar capacidade de armazenamento de carbono orgânico nos habitats amostrados até uma profundidade máxima de 1 metro de profundidade. As assinaturas isotópicas ($\delta^{13}C_{org}$ e $\delta^{15}N_{total}$) foram analisadas com um modelo de mistura de isótopos estáveis para estimar a origem da matéria orgânica no sedimento de *Z. noltei* e *S. maritima*. Nestas estações de amostragem,

os conteúdos de carbono orgânico, as capacidades de sequestração e contribuições das fontes de matéria orgânica foram comparadas ao longo do gradiente hidrodinâmico e entre habitats. A vegetação nas estações ao longo do gradiente hidrodinâmico foi descrita relativamente à densidade de rebentos, altura da vegetação, área da copa, biomassa aérea e biomassa subterrânea. As diferenças entre as propriedades da vegetação foram analisadas entre estações e espécies. Por fim, modelos para a estimativas dos conteúdos elementares (carbono orgânico e azoto total) com base no conteúdo de matéria orgânica, bem como a estimativa da matéria orgânica com base na cor de sedimento foram propostos.

Os perfis sedimentares descritos nos locais suportam a importância da variação de hidrodinâmica ao longo das estações de amostragem, sendo observado um aumento progressivo da fração de argila e lodo no sedimento com a redução da hidrodinâmica à qual a estação está exposta. No sedimento da estação do viveiro de amêijoas, o sedimento era quase totalmente areia, exceto uma pequena camada de lama que possivelmente terá sido formada durante o período em que este local não foi explorado. Foram encontradas diferenças entre os armazenamentos de carbono (por área) entre as áreas vegetadas (*Zostera noltei* e *Spartina maritima*) e o viveiro de amêijoas. Esta diferença era esperada e deve-se ao distúrbio constante a que o sedimento superficial é submetido, bem como a constituição do sedimento (areia) que promove taxas de decomposição mais elevadas neste local. Os armazenamentos de carbono dos habitats *Z. noltei* e *S. maritima* não diferiram e encontraram-se abaixo das atuais estimativas globais de armazenamento nestes habitats. Os conteúdos de carbono orgânico (em percentagem de peso seco) diminuíram continuamente ao longo da profundidade nas 8 estações de *Z. noltei* e *S. maritima*, indicando degradação contínua da matéria orgânica ao longo do tempo. Nas 2 estações mais expostas à hidrodinâmica, esta diminuição foi menos acentuada e os valores de conteúdo de carbono médios foram mais baixos do que nas 2 estações mais abrigadas. Esta diferença poderá indicar diferentes taxas de degradação da matéria orgânica, ou refletir diferenças em taxas de sedimentação e sequestração de matéria orgânica. As contribuições das fontes de matéria orgânica sugerem que a origem da matéria orgânica nestes dois habitats não difere muito, sendo os principais contribuidores matéria orgânica particulada suspensa, seguido de produção primária nestes habitats (tecido vegetal de *Z. noltei* e *S. maritima*). A contribuição do tecido vegetal de *Z. noltei* e *S. maritima* nas pradarias de ervas marinhas aumentou com a diminuição da hidrodinâmica, sugerindo

que existem diferenças nas taxas de exportação de produtividade primária neste habitat, em função da energia à qual a pradaria está exposta. Por fim, a matéria orgânica mostrou ser um bom estimador para conteúdos elementares (C_{org} e N_{total}), sendo que esta relação não variou significativamente entre habitats.

Em conclusão, este trabalho reforça a importância da utilização de dados representativos ao estimar armazenamentos de carbono nestes habitats. Grandes discrepâncias são encontradas entre as espécies usadas para estimar médias globais, fazendo com que estimativas com base nestes valores tenham uma grande probabilidade de sobre/subestimar os armazenamentos. As diferenças encontradas dentro de um habitat com base na hidrodinâmica do local mostram também a importância de tentar incluir parâmetros abióticos nestas estimativas, de modo a melhorar a sua exatidão. Com variações em stock de carbono

Palavras chave: pradarias de ervas marinhas; Ria Formosa; sapais; sequestro de carbono orgânico; serviços ecossistémicos.

Table of contents

Table of figures

1 INTRODUCTION

1.1 Ecosystem services

Ecosystem services can be broadly defined as natural processes and components that benefit human well-being. These ecosystem services provide a broad range of benefits, normally classified under four categories: provisioning, regulating, supporting and cultural (Millennium Ecosystem Assessment, 2005). Over the past decades, changes in land use, loss of biodiversity, population overexploitation and others have caused degradation of these ecosystem services, leading to a decreased quality of life for human populations that benefit from them, as well as significant costs for ecosystem services that require anthropogenic action to be replaced. (Costanza et al., 2014; Sutton et al., 2016).

Monetization of ecosystem services and their entrance into the market has been the most effective strategy to influence management decisions. By including ecosystem services in cost-benefit analysis, it was concluded that increasing an ecosystem's sustainability can often bring economic benefits that outweigh those of increased exploitation (Millennium Ecosystem Assessment, 2005). The downside of this management system is that nonmarketed ecosystem services (without monetary value estimations) will often be ignored and degraded. This makes an effective study to identify, quantify and market ecosystem services a priority to increase effectiveness of policy making (Kubiszewski et al., 2017; Maes et al., 2012; Sutton et al., 2016).

1.2 Atmospheric carbon and natural carbon sinks: the blue carbon strategy

Anthropogenic emissions of green-house gases (GHG) are currently at the highest levels in history. These emissions are associated with environmental changes that could irreversibly alter the climate in our planet (IPCC, 2014). Effects of climate change will include higher average temperatures, more common and longer heat waves, sea level rise, changes in precipitation patterns and ocean acidification. These pose a danger to human society and have brought a growing interest towards measures to slow and mitigate them. In order to minimize impacts, a substantial decrease in GHG emissions is required (IPCC, 2014). The major contributor to GHG emissions is carbon dioxide (CO_2), comprising 76% of all emissions (IPCC, 2014). Given that methods of CO_2 removal from the atmosphere

have prohibitively high prices, attention is turning into the protection of terrestrial and aquatic ecosystems that have a natural high potential of carbon sequestration, a regulating ecosystem service. These measures aim to not only promote sequestration of atmospheric carbon, but also to protect carbon stocks already in place (Duarte et al., 2013b; Trumper et al., 2009)

The idea of including ecosystems that act as carbon sinks in climate change mitigation policies is referred to as Green and Blue carbon strategies, when referring to terrestrial and marine habitats, respectively (Nellemann et al. 2009). Coastal vegetated areas (salt marshes, mangroves and seagrass meadows) are recognized as particularly efficient oceanic carbon sinking areas. Despite covering less than 0.5% of the world's sea bed, these areas are responsible for more than half of the carbon stocks in oceanic sediments, (Fourqurean et al., 2012; Marbà et al., 2015; McLeod et al., 2011; Nellemann et al., 2009). As such, the Blue Carbon strategies focus on coastal vegetated habitats, trying to identify and understand the environmental drivers behind the carbon sequestration potential of these areas. Hopefully, this will allow a more effective application of Blue Carbon strategies and facilitate management decisions regarding these high carbon ecosystems, with the goal of protecting and restoring the natural habitats currently in place that promote removal of atmospheric CO_2. It should be noted that the Blue and Green carbon strategies do not aim to replace other strategies such as carbon emissions reduction, but to complement them (Nellemann et al., 2009).

1.3 Carbon accumulation and sequestration in coastal vegetated areas

1.3.1 Organic matter fluxes and controls

Seagrass meadows and saltmarshes are recognized as highly productive ecosystems, providing valuable services. This is due to an agglomerate of primary producers that exist in these complex ecosystems, comprising not only seagrasses/ saltmarsh plants, but also epiphytes and phytobenthos (Gacia & Duarte, 2001; Nellemann et al., 2009). Furthermore, the carbon sequestered to sediment in these areas is not exclusively produced *in situ* (i.e. autochthonous organic matter). Rather, the high efficiency of seagrass meadows and saltmarshes in sequestering carbon is partially attributed to their ability to trap allochthonous organic matter (Dahl et al., 2016b; Mateo et al., 2006).

The stocks of organic matter (OM) and organic carbon in a coastal vegetated ecosystem can be summarized in 3 categories: plant biomass, labile detrital biomass and refractory detrital biomass (Figure 1.1). Carbon in the first two categories usually represents short/medium term sequestration, while carbon in refractory detrital mass is sequestered for long term, up to millennia in some species (Mateo et al., 1997). In coastal vegetated habitats, detrital biomass that has been sequestered in the sediment represents the most significant OM stocks (Cebrian, 1999; Dahl et al., 2016b; Fourqurean et al., 2012; Serrano et al., 2016b).

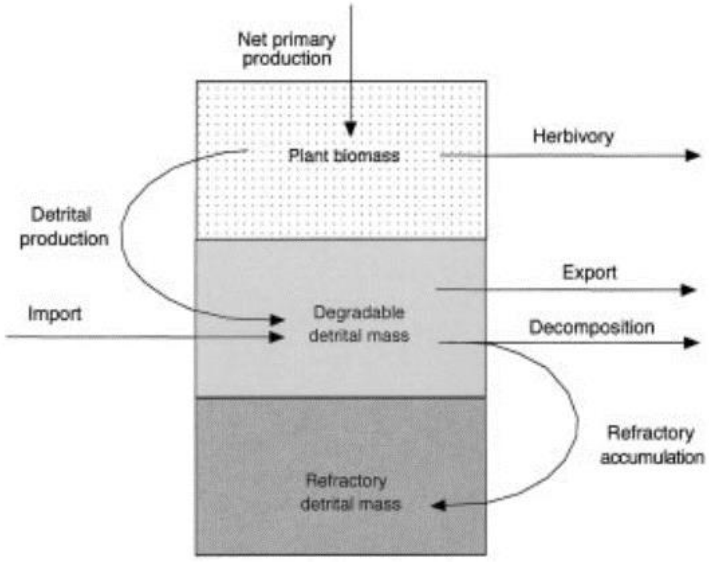

Figure 1.1 – Fate of primary production and compartments of organic matter stocks in coastal vegetated ecosystems. Plant biomass increases due to net primary production and decreases due to herbivory. Part of that production is transferred to degradable detrital mass. The labile detrital mass compartment can also be increased by organic matter importation, while exportation and decomposition decrease it. Lastly, part of the degradable detrital mass is buried accumulated in the sediment in the refractory detrital mass, forming stocks that can last up to millennia (source: Cebrian, 1999).

The refractory (long-term) OM stocks of a meadow/saltmarsh will be determined by the amount of the labile detrital OM and fraction of that OM that is sequestered to the sediment (Mateo et al., 2006). The stocks of labile detrital OM are increased mostly by two factors (inputs of OM): sequestration of autochthonous OM and allochthonous OM importation.

Autochthonous OM deposition rates are dependent on primary productivity and exportation of OM. Exportation of OM is a crucial factor when considering carbon flow in seagrass meadows and saltmarshes. However, quantifying exportation rates is difficult due to the open nature of these ecosystems. Exportation is more significant for above

ground biomass and estimates are highly variable, ranging from 0 to 100% (Mateo et al., 2006). The main factor that dictates exportation rates is the intensity of physical energy over the bed, which is dependent on the water currents and waves forcing the meadow. In high energy environments, the release and transport of OM from the canopy to adjacent areas, as well as the resuspension rate, increase. (Bach et al., 1986; Mateo et al., 2003). Another impactful factor is the leaf structure. Some species have bulky leaves that sink almost immediately after shedding, whereas others have leaves that will float for longer periods of time due to internal aerenchymas. Leaves that take longer to sink have an increased probability of being exported, leading to a decreased contribution from the autochthonous OM (Mateo et al., 2006).

The importation of allochthonous OM to the degradable detrital biomass compartment will depend mostly on OM deposition rates. Coastal vegetated areas are known for high deposition rates due to the impact of vegetation on hydrodynamics, as well as particle momentum. Seagrass meadows and saltmarshes reduce flow and turbulence, promoting particle sedimentation and reducing resuspension (Duarte et al., 2013b; Hendriks et al., 2008; Kennedy et al., 2010). Particles can also be directly affected by reducing particle momentum and increasing path lengths due to collisions with the canopy (Hendriks et al., 2008). Once settled, fine sediments are trapped by the colloidal structure of surface sediments (Friend et al., 2003). This process promotes not only an increased deposition of particles in general, but most importantly of fine sediment particles. Fine sediment particles are associated with organic matter due to sorption processes, where OM is found on the sediment grains in layers, meaning that sediment with higher area to volume ratios can transport a higher amount of OM (Bianchi, 2007). The combination of high productivity and high sediment deposition rates (fine sediment in particular) leads to a higher ability to sequester carbon in vegetated coastal habitats, than in unvegetated ones (Dahl et al., 2016a).

The fraction of short-term stocks that is buried, is determined mostly by short-term decomposition. This process is the most likely fate for both above and below ground seagrass biomass, with estimations that 15% to 95% of seagrass production is degraded in short-term and recycled by the ecosystem (Mateo et al., 2006). Detrital organic matter in the superficial sediment that is not quickly degraded or exported will be buried deeper over time, entering the refractory organic matter pool (Figure 1.1). The main controls for the fraction of the short-term stocks that are sequestered in a long-term basis are

composition of the organic matter (how labile/refractory it is) (Serrano et al., 2016b) and burial rate of the OM, with quicker burial rates leading to faster creation of anoxic conditions and reducing the efficiency of the degradation process (Bianchi, 2007).

Even when OM has entered the refractory OM pool, the degradation process still continues. However, it occurs at a relatively slow rate depending on the balance between microbiotic communities, environmental conditions (temperature, oxygenation, water nutrient content and desiccation) and the liability/refractance of the OM (Harrison, 1989; Serrano et al., 2016b). There are a few factors that promote a slow degradation of OM stocks in coastal vegetated areas: 1) Seagrass tissues going through an initial leaching process that results in OM poor in inorganic nutrients and with a high fraction of cellulose and lignin (Harrison, 1989); 2) Accumulation of fine sediments leading to low sediment oxygenation/ redox potentials in the sediment column; 3) High concentration of organic matter accelerating oxygen consumption causing anoxia conditions (Cebrian, 1999; Mateo et al., 2006; Serrano et al., 2016b). It is thus the combination of high OM accumulation rates and slow degradation rate of the refractory detrital mass that promotes the large carbon stocks that are often found in the sediment beneath the seagrass meadows/ saltmarsh areas (Dahl et al., 2016a; Koho et al., 2013; Mateo et al., 2006; Serrano et al., 2016b).

1.3.2 Carbon stocks in coastal vegetated areas

Current knowledge on carbon stocks estimations for seagrass meadows suggests that a large variability exists, both amongst locations and species (Fourqurean et al., 2012; Lavery et al., 2013). In Australian seagrass species, C_{org} storage was found to vary, on average, from 0.03± 0.01 g C_{org} cm^{-2} to 0.48 g C_{org} cm^{-2} in the top 24 cm, with an 18-fold difference amongst the minimum and maximum measured values (Lavery et al., 2013). For *Z. marina*, carbon storage in the top 25 cm of meadows located in different sites ranged from 0.05 ± 0.005 g C_{org} cm^{-2} to 0.35 ± 0.041 g C_{org} cm^{-2} (Dahl et al., 2016a). A review of global carbon storage data for the top 1 meter of the sedimentary column reported values of 1.15 g C_{org} cm^{-2} to 8.29 g C_{org} cm^{-2}, with a mean value of 3.29 ±0.56 g C_{org} cm^{-2} (Fourqurean et al., 2012).

Saltmarsh organic carbon storage data also suggests a high variability in the top meter of sediment. In Australian tidal marshes, C_{org} storage estimates range from 0.91 ± 0.10 g C_{org} cm^{-2} to 1.88 ± 0.09 g C_{org} cm^{-2}, with differences being driven both by species

and abiotic factors (Macreadie et al., 2017). A study in southeastern Australian saltmarshes reported an average of 1.65 ± 0.09 g C_{org} cm^{-2}, with measures between 0.18 g cm^{-2} and 4.48 g C_{org} cm^{-2} (Kelleway et al., 2016), with global estimates reporting a mean storage of 1.62 g C_{org} cm^{-2} (Duarte et al., 2013b).

Despite more data on carbon stocks and storage in these habitats becoming available recently, there are still some problems with current values that can lead to errors in estimations: 1) Lack of information on how the carbon storage changes along a species' geographic distribution (Macreadie et al., 2017; Ricart et al., 2015); 2) Lack of data on differences in carbon storage due to variation in abiotic factors, making it hard to include them in estimations/models (Dahl et al., 2016a; Kelleway et al., 2016; Serrano et al., 2016b); 3) Overrepresentation of certain areas (such as the Mediterranean and Australia), while information in places such as the African continent is lacking (Fourqurean et al., 2012; Miyajima et al., 2015). 4) Overrepresentation of data on some species, particularly in the *Posidonia* genus (Duarte et al., 2004; Fourqurean et al., 2012; Kennedy et al., 2010), a genus known to sequester higher amounts of carbon than the average seagrass species (Lavery et al., 2013). In addition, most of the studies on carbon stocks focus on a single habitat (seagrass or saltmarsh), while they normally co-occur in many areas. Finally, the contribution of macroalgae habitats in terms of carbon sequestration is also underrepresented. Having a comparison of the contribution of different coastal vegetated ecosystems to the "blue carbon" will allow a better understanding of their role in the global C cycle and in the mitigation of climate change.

In order to contribute to fill some of those gaps, this thesis aims to study the carbon storage in the Ria Formosa, a coastal lagoon where seagrasses, saltmarsh and subtidal macroalgae and human-altered areas, co-occur. This will allow us to have allow better regional estimations of carbon stocks than simply relying on global estimates. Studying how this carbon storage varies due to hydrodynamics, an important abiotic factor in the lagood, could allow even further refinement of those estimations. The comparison of these carbon storage in these vegetated habitats to carbon storage in clam farms is relevant to better understand and weight the cost-benefits of converting these habitats. Increasing carbon storage knowledge in some of the less studied species, such as *Zostera noltei* (a short-living seagrass species and the most common one in the Ria Formosa) is also needed to increase accuracy of carbon stored in these habitats across the globe. Accuracy of those estimates is of important to understand their role in the carbon cycle and ensure that policy

and decision making is based on reliable data (Johannessen & Macdonald, 2016; Maes et al., 2012).

1.4 Organic matter provenance: Stable Isotope Mixing Models

Organic matter stocks in the sediment are a mixture of OM originating from several sources. The contribution of those sources can be estimated using Stable Isotope Mixing Models (SIMMs), based on the isotopic signatures of both sources and mixtures. While initially simple, these models have become more sophisticated and are now being used several purposes, such as estimating the contribution of different sources to sedimentary organic matter stocks in seagrass meadows (Kennedy et al., 2010; Macreadie et al., 2012; Marbà et al., 2015; Serrano et al., 2016b; Watanabe & Kuwae, 2015). Some of the most recently added features in the models are: 1) ability to account for variability in mixture and source signatures to estimate uncertainties, rather than point estimates; 2) accounting for large discrepancies in elemental concentrations of the sources by adding concentration-dependency; 3) estimating contribution of a large number of sources, as opposed to n+1 sources, where n is the number of isotopes being analyzed (Parnell et al., 2013; Phillips & Gregg, 2003; Phillips et al., 2014)

To calculate contributions of various sources to a mixture, stable isotope signatures are expressed in delta notation as per mil. These are calculated as follows:

$$\delta X(‰) = \left(\frac{R_{sample} - R_{standard}}{R_{standard}}\right) \times 1000$$

$$R = \frac{\text{Heavy isotope}}{\text{Light isotope}}$$

$R_{standard}$ corresponds to the ratio of heavy to light isotopes in a specific sample that is used internationally for comparison and depends on the element being analyzed (Kennedy et al., 2010). These models then calculate the contributions of each source by assuming that the isotopic signature of a mixture is equal to the sum of the sources' signatures times their contribution. They also assume that the sum of contributions adds to 1 (Hopkins & Ferguson, 2012).

Previous studies that estimated contribution of organic matter sources to sediment in seagrass meadows and saltmarshes found a large range of contributions. In *Z. marina* meadows, Röhr et al. (2016) reported that autochtonous organic matter contributed between 2 and 80% of the OM in the sediment, with the other major contributors being

phytoplankton and algae. It's hypothesized one of the factors in *Z. marina* contribution variability is the exposure of the meadows, with more exposed meadows exporting more primary production. A study performed on 5 species found that in tropical seagrass meadows on carbonate sediments, 35 to 82% of organic carbon derived from seagrasses. In temperate and tropical meadows, the contribution ranged from 4 to 40%. A review of 207 seagrass meadow sites worldwide estimated that the in average, approximately 50% of organic carbon buried in seagrass meadow sediment originates from seagrass production (Kennedy et al., 2010).

1.5 Sediment color

The color of the sediment is affected by several of its properties. It has been used in the field to roughly estimate organic matter content, as well as estimating some of the main minerals and biochemical processes present in it (Bigham et al., 1993; Wills et al., 2007; Zelenak, 1995). Methodologies already exist to estimate organic matter content from color, focusing mostly on the darkness of the sediment. In general, the darker the sediment, the higher is the organic matter content. Many of these methodologies relied on subjective color evaluation by the technician, leading to large errors in estimations (Zelenak, 1995). The usage of color measuring instruments (spectrophotometers) improved the consistency of color measurements and the accuracy of OM predictions based on sediment color (Zelenak, 1995).

Thus, if sedimentary organic carbon and organic matter are correlated, the color of the sediment could be used as a proxy for the organic carbon stock in different habitats. Despite this straight potential application, the usefulness of the sediment color has not been investigated yet in sediments of coastal vegetated areas for rough estimations of C stocks. This is worthy of investigating since color measurements require less labor, a simpler process and are done using cheaper equipment than direct determination of organic carbon.

1.6 Objectives and hypothesis

There is a growing concern to understand the fundaments and mechanisms of carbon sequestration in vegetated coastal ecosystems. The general objective of this thesis is to contribute to the understanding of the factors affecting the carbon stocks' size in

coastal vegetated areas with emphasis in the role of the hydrodynamics regime and habitat type. For that purpose, different ecosystems (seagrass meadow, saltmarshes, macroalgal beds and clam farm) in the Ria Formosa lagoon (Southern Portugal) will be used as a case study.

The specific objectives of this study, and respective hypothesis, are:

1) **Objective:** To describe the sedimentary profile beneath intact and human-modified coastal vegetated areas in the Ria Formosa lagoon;

   Hypothesis: The human-modified area (clam farm) is expected to be comprised of higher sand contents than intact vegetated areas due to seagrass removal and sand addition performed to create the farms. The fraction of coarse sediment is also expected to be higher in areas subjected to high hydrodynamic energy, than those that are sheltered, since low energy environments promote the sedimentation of fine particles.

2) **Objective:** To quantify and compare the C_{org} storage capacity of intertidal seagrasses (*Zostera noltei*), saltmarshes (*Spartina maritima*), macroalgae subtidal meadows (*Caulerpa prolifera*), and human-modified areas (clam farms) in the Ria Formosa lagoon;

   Hypothesis: Carbon storage is expected to be lower in the clam farm due to the lack of vegetation that acts as promotor of organic matter sedimentation. Regarding seagrass, saltmarsh and macroalgae beds, the carbon stocks may depend on the properties of the vegetation and their position along the shore.

3) **Objective:** To investigate how the hydrodynamic regimes influence the C_{org} storage of intertidal seagrasses (*Zostera noltei*) and saltmarshes (*Spartina maritima*), and investigate the contribution of allochthonous and autochthonous sources to the sedimentary C_{org} stocks in the two habitats.

   Hypothesis: Carbon storage is expected to be higher in stations with low hydrodynamics for being areas of sedimentation of fine particles, which promote the adhesion of organic matter and a slower decomposition rate. Contribution of allochthonous matter is also expected to be higher in stations with low hydrodynamics due to lower exportation the primary production.

4) **Objective:** To investigate sediment variables (OM and color) to use as proxy of the sedimentary C_{org} stock.

   Hypothesis: Organic matter is expected to be a very strong predictor for organic carbon and total nitrogen contents. Sediment color (particularly Lightness, i.e a measure in a grey-scale) is expected to be somewhat predictive of organic matter contents (the darker the sediment, the higher the organic matter content).

2 METHODOLOGY

2.1 Study site

The Ria Formosa is a coastal lagoon system on the South coast of Portugal, with a surface area of ca. 118 km^2 (Ceia, 2009). It is separated from the ocean by 3 barrier islands and 2 peninsulas. Due to its strong mesotidal regime (with an amplitude of approximately 3.5m) (Ceia, 2009), many of the sand banks are dominated by intertidal habitats. Upper tidal areas are dominated by saltmarshes (mainly *Spartina maritima*) that flood during high tide, while lower tidal areas are vegetated by seagrass meadows (mainly *Zostera noltei*) that become exposed during low tide (Arnaud-Fassetta et al., 2006; Guimarães et al., 2012). The lagoon's main hydrodynamic energy input is the tide, with 4 main inlets: Ancão, Faro, Armona and Tavira. These inlets lead into the main channels, which will separate into several tributary channels of calmer hydrodynamic regimes (Ceia, 2009).

Four sampling stations were selected along a bank near the Faro inlet, beginning in the main navigation channel (station 1) and leading into a tributary channel (stations 2 to 4) (Figure 2.2). The distance of the stations to inlet was used as a proxy for hydrodynamic regime, and varied between 2.49 km (station 1) and 4.71 km (station 4) (Table 2.1). Analysis of superficial sediment granulometry previously performed at the stations showed a trend of increasing fine sediment fraction from station 1 to station 4 (Núñez, 2015). This trend supports the existence of a hydrodynamic gradient along the defined stations. In each station, sampling was conducted in meadows of two species: seagrass *Zostera noltei* (ZN) and saltmarsh species *Spartina maritima* (SM).

A clam farm (CF) was selected as representative of human-modified coastal vegetate areas, since the Ria Formosa is substantially modified by this activity (Guimarães et al., 2012). Clam farming at the selected location began near 1920. The activity was temporarily stopped around 1960 but resumed in 2000 and has occurred continuously since then. Finally, an area that has been recently colonized by *Caulerpa prolifera* (CA) was also included, being only subtidal sampling location. The total of 10 sampling stations are named after the species they represent plus a number given to the station (e.g. ZN1; SM3; CA) and cores will be in the same way.

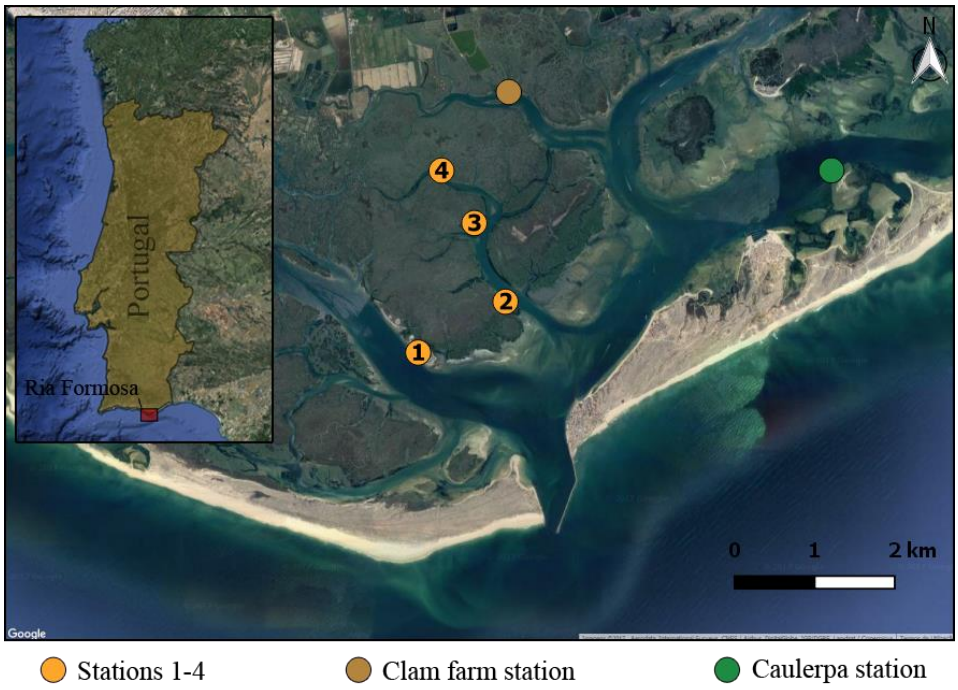

Figure 2.2 - Location of the sampling stations in the Ria Formosa, South Portugal. Stations 1-4 included sampling in *Zostera noltei* and *Spartina maritima*.

Table 2.1 - Geographical description of the sampling stations. ZN: *Zostera noltei*, SM: *Spartina maritima*, CA: *Caulerpa prolifera*, CF: *Clam Farm*.

Station	Distance from Faro inlet (km)	Latitude	Longitude
ZN/SM - Station 1	2.49	36° 58' 58.5610" N	-7° 52' 31.3140" W
ZN/SM - Station 2	2.66	36° 59' 19.0734" N	-7° 52' 32.9606" W
ZN/SM - Station 3	3.68	36° 59' 50.7664" N	-7° 52' 48.6952" W
ZN/SM - Station 4	4.71	37° 00' 11.9322" N	-7° 53' 05.2382" W
CA	-	37° 00' 12.0060" N	-7° 49' 48.4248" W
CF	-	37° 00' 43.5798" N	-7° 52' 31.3140" W

2.2 Vegetation's properties

A description of the ZN and SM stations was performed during a 1-day campaign (13th of January 2017) at low tide. Vegetation properties determined for *Z. noltei* and *S. maritima* were: shoot density (shoots m^{-2}), canopy height (cm), above-ground biomass (g DW m^{-2}), below-ground biomass (g DW m^{-2}) and an index of the canopy area per unit of

sediment surface area, *i.e.* the leaf area index (LAI, for ZN) and LAI plus stem area (for SM).

Replicated quadrates (n = 3) were haphazardly positioned in each sampling location and vegetation in the corresponding area was extracted, ensuring that all the tissue below and above ground was included. The area of the quadrats was selected based on the species being sampled: *Z. noltei* = 10×10 cm (100 cm^2); *S. maritima* = 28×28 cm (784 cm^2). Tissue samples were rinsed of sediment in situ and brought to the laboratory, where they were frozen at -20ºC until processing.

When processing samples, vegetal tissue was repeatedly rinsed and manually selected until all material not belonging to the target species had been removed. Total number of shoots was counted and five shoots were selected to measure total length and area. Areas were measured by scanning followed by image processing in ImageJ1.51n (Schneider et al., 2012). LAI and stem areas could then be calculated as:

(1) **Leaf area index (m^2 m^{-2})** = Leaves per shoot × Shoot density (shoots m^{-2}) × Shoot area (m^2 shoot)

(2) **Stem area (m^2)** = π × Projected stem area (m^2)

Biomass was then separated in above ground (leaves for ZN, leaves + stems for SM) and below ground (roots and rhizomes), dried in an oven at 60ºC until constant weight (4 to 5 days) and weighted (dry weight, g DW).

2.3 Organic matter sources collection

Samples of the potentially most important sources of organic matter to these ecosystems were collected during January and February of 2017. Four main sources were selected: suspended particulate organic matter (SPOM), *Z. noltei* tissue, *S. maritima* tissue and macroalgae that formed mats in both areas (*Ulva* sp. plus epiphytes).

SPOM samples were obtained by collecting 1 L of superficial seawater near each station, in the middle of the channel. Water samples were filtered using a vacuum pump system through glass microfiber filters (GF/F, 47 mm). After sample filtration, filters were rinsed with distilled water to remove salts and ensure that all particles were removed

from the filtration cup. Filters were carefully removed and stored in identified petri dishes which were frozen at -20ºC, lyophilized for 24 hours and stored until further analysis.

Replicated samples (n = 3) of *Z. noltei* and *S. maritima* were cleaned of epiphytes and sediments, rinsed with distilled water, separated into above and below-ground tissues and then frozen (-20ºC) until sample processing. Later they were lyophilized for 24 hours, pulverized in a ball-mill (with agate material to avoid contamination) and sent for elemental and isotopic analysis.

2.4 Core extraction, description and sub-sampling

Sediment cores were extracted from the sampling locations from 30 of January to 16 of February of 2017. An area within the vegetation patch was selected to avoid edge effects. Core samplers consisting of sharpened PVC pipes (length = 170 cm; ø = 5cm) were manually hammered into the seafloor until penetration was no longer possible, or a depth of 160 cm was reached. The difference between the core sampler's upper mouth and the seafloor was measured (extra – e) for further calculations (Figure 2.3). A styrofoam plug was then inserted in the upper part of the sampler until the surface of the sediment core was reached and the sampler was sealed at the top (using a rubber stopper) to restrict air flow. A raised pulley system supported in platforms was used to extract the core. Bottom of the sampler was checked for any loss of sediment during the uplift and the height of the amount lost (lost – L, Figure 2.3) was measured with a ruler. Sediment cores were transported carefully to the laboratory for immediate processing.

In the laboratory, core samplers were longitudinally cut in half using a mechanical saw and cores were halved with a wire saw. The height of the sediment core was measured (height – h, Figure 2.3) with a metric tape (±0.1 cm).

Core compaction was visually appreciable during its extraction. The compaction rate was calculated for each core assuming linear compression (equation 8) (Glew et al., 2001) based on the measures taken during core extraction. All measured volumes and depths along each core were corrected by dividing them by the compaction correction factor (equation 7) of that specific core.

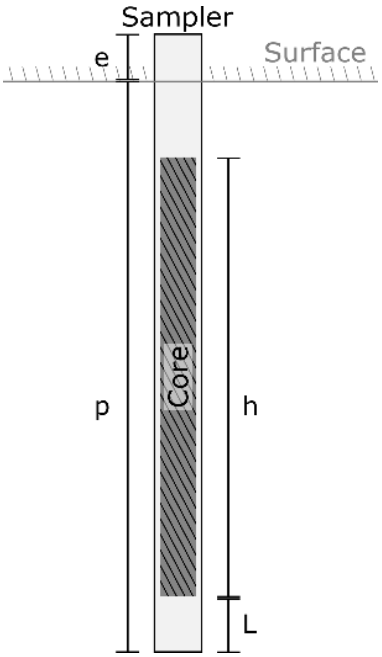

Figure 2.3 - Schematic of measurements used to calculate and correct compaction.

(3) **Penetration depth (p) (cm)** = 170 – e

(4) **Compaction correction factor (C_{corr})** = $\frac{h+L}{p}$

(5) **Compaction rate** = $(1 - C_{corr}) \times 100$

One half of the core was photographed and visually described by determining layers of similar sediment lithology and horizons delimiting such layers. Presence of organisms and organic structures was also noted (symbology adapted from Li et al. 2015). Sediment color measurements (n = 3) were performed every 1 cm using an X-Rite Colortron II spectrophotometer, after covering the core surface in plastic wrap to prevent sediment from adhering to the equipment (no significant effect of plastic wrapping on color measurements has been proved in preliminary tests). The core was then sliced and sub-sampled every 2 cm using a Teflon spatula. During sampling, the sediment near the corer was avoided to prevent potential contamination by transported materials along the sampler walls during the core extraction. Samples were placed in identified zip-lock bags and frozen at -20ºC until further processing (group A samples).

The second core half was also divided in slices every 2 cm. First, a sub-sample from each slice was taken using a syringe (diameter of 1.5 cm). Volume of the sample (Sample Volume, cm^3) was measured in the syringe graduation (±0.1 mL) and the sample was placed in an identified zip-lock bag (group B samples). The remaining sediment in the slice was sampled into a separated zip-lock bag (group C samples). All samples were then frozen at -20ºC for storage.

2.5 Sediment properties analysis

2.5.1 Sample selection

A series of samples along each core was selected for further analysis. Two selection criteria were used, based on the depth of the samples:

a) Samples in the top 50 cm of depth: select every other slice;

b) Samples over 50 cm of depth: select the second sample before and after each horizon, so that the start and end of each sedimentary layer were measured. If a layer was over 30 cm long, a middle sample was also selected. Layers under 5 cm of length were disregarded. When samples with high content of shell fragments were selected, another sample was selected deeper within the layer.

2.5.2 Porosity, dry bulk density and organic matter fraction

Porosity, dry bulk density (DBD) and organic matter fraction were determined in sub-samples B. Because these are flooded sediments, porosity (equation 7) and DBD can be determined based on the moisture content (Avnimelech et al., 2001). Frozen samples were weighted ($Weight_{initial}$, g) in a micro-balance (±0.0001 g), lyophilized (24 h) and weighted again ($Weight_{dry}$, g). The DBD was calculated as the ratio between the dry weight and the sample volume (equation 7).

(6) $$\textbf{Porosity (\%)} = \frac{\mathrm{Weight_{initial}(g) - Weight_{dry}(g)}}{\mathrm{Weight_{initial}(g)}} \times 100$$

(7) $$\textbf{Dry bulk density (g cm}^{-3}\textbf{)} = \frac{\mathrm{Weight_{dry}(g)}}{\mathrm{Sample\ Volume(cm^3)}}$$

Sediment samples were then ground in a ball mill using agate material until a fine and homogenous powder was obtained. Approximately 0.5 g of the ground samples were stored in identified Eppendorf tubes for isotopic analysis. The remaining ground sample was weighted ($Weight_{dry}$, g), placed in an aluminum foil cup and used to estimate the organic matter content by Loss on Ignition (LOI) (equation 8), I.e. by combusting the sample at 450ºC for 4 hours (Heiri et al., 2001).

(8) $$\textbf{Organic matter content (\%)} = \frac{\text{Weight}_{\text{dry}}\ (\text{g}) - \text{Weight}_{\text{combusted}}\ (\text{g})}{\text{Weight}_{\text{dry}}\ (\text{g})} \times 100$$

The OM content and DBD were then used to calculate the sediment OM concentration (equation 9), which gives the amount of OM per unit of sediment volume.

(9) $$\textbf{OM concentration (g OM cm}^{-3}\textbf{)} = \text{OM content}\ (\%) \times \text{Dry Bulk Density}\ (\text{g cm}^{-3})$$

2.5.3 Elemental and isotopic analysis

Organic carbon content (C_{org}, % dry weight) and $\delta^{13}C_{org}$ (vs VPDB) were analyzed in the sediment samples after carbonate removal by direct addition of 1 M HCl until the reaction was complete. Total nitrogen content (N_{total}, % dry weight) and $\delta^{15}N$ (vs Air) were analyzed in untreated samples. Isotopic signatures were also analyzed in the dry tissues of the sources selected for the mixing models (section 2.3). Organic carbon content analysis was performed by high temperature combustion NDIR detection (method reference: EPA 415.1; instrument: Shimadzu TOC-V). Total nitrogen content was analyzed by high temperature combustion chemiluminescence detection (method reference: ASTM D5176; instrument: Shimadzu TNM-1). Both $\delta 13C_{org}$ and $\delta 15N$ were analyzed by Isotope Ratio Mass Spectrometry (instrument: Thermo DeltaV). Sample treatment and analysis was performed by UH Hilo Analytical Laboratory (Hawaii, USA). Values of elemental concentrations under detection limit were assumed to be 0.

Organic carbon and total nitrogen contents were used in conjunction with dry bulk density to calculate sediment C_{org} and N_{total} concentrations (g element cm-^{3}, equation 10).

(10) $$\textbf{Element concentration (g element cm}^{-3}\textbf{)} = \text{element content} \times \text{DBD}$$

C_{org} and N_{total} concentration were integrated along the core depth (standardized to 100 cm) to calculate the storage capacity of each habitat (g element cm^{-2}), i.e. the C_{org} or N_{total} stock per area. Approximate integral values were calculated using linear interpolation (Ekstrøm, 2017).

2.6 Stable Isotopic Mixture Models

Stable isotopic mixture models were calculated using SIMMR library from R (Parnell, 2016), utilizing four main sources of organic matter: suspended particulate organic matter (SPOM); macroalgae (MA), *S. maritima* (SM) and *Z. noltei* (ZN).

Samples that were considered to have suffered changes in signatures due to diagenesis were excluded. This evaluation was performed separately for carbon and nitrogen: 1) low C_{org} contents were associated with a lower $\delta^{13}C_{org}$, suggesting that degradation of organic matter in those samples affected $\delta^{13}C_{org}$; 2) low N_{total} was related to an increase in the variance of $\delta^{15}N$, once again suggesting possible alterations due to organic matter degradation. Samples with the largest alterations were excluded in both cases (i.e low $\delta 13C_{org}$ plus low C_{org} content; low N_{total} content plus high deviance from mean value) (Annex 1).

2.7 Sediment color

Sediment color was measured and analyzed in CIELab color space. Designed to be in accordance with the Munsell color system typically used for soil characterization (Koschan & Abidi, 2008; Wills et al., 2007), this system characterizes colors using three dimensions: lightness (L*, where 0 equals to black and 100 equals to diffuse white); red-green (a*, negative values correspond to green, positive values correspond to red); yellow-blue (b*, negative values correspond to blue, positive values correspond to yellow)(Figure 2.4) (Adobe Systems Incorporated, 2000).

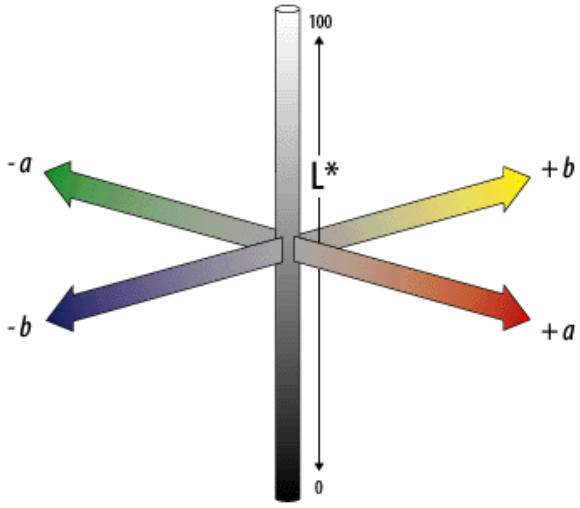

Figure 2.4 - CIELAB color space dimensions. The color space uses 3 dimensions to describe color: L* (lightness); a* (green-red) and b* (blue-yellow). (Adobe Systems Incorporated, 2000).

2.8 Statistical analysis

2.8.1 Vegetation description

Differences of vegetation parameters amongst stations (1 to 4) within each habitat (ZN and SM), or differences between habitats (ZN and SM) were tested by one-way ANOVA (when assumptions of normality and homoscedasticity were met) or Kruskall-Wallis (when assumptions were not met). Differences between groups were tested using TukeyHSD multiple comparison test (for ANOVA) or Dunn's test (for Kruskall-Wallis). Effects were considered significant at $p < 0.05$.

2.8.2 Sedimentary C_{org} content

Stepwise regression analysis (bidirectional elimination) was performed to select the best model to predict C_{org}. The full model included Habitat, Station, Depth, Habitat:Depth interaction and Station:Depth interactions. Another analysis with $\log_{10}$-transformed Depth was also done. Addition and removal of predictors was performed and subsequent model performance was compared based on AIC (Akaike Information Criterion, Akaike (1974), with the lowest AIC corresponding to the best model). Pair-wise comparisons were performed on the marginal means of the selected model to test for significant differences C_{org} contents between sampled cores (Tukey's HSD). Differences were considered significant at $p < 0.05$.

2.8.3 Organic matter sources

The effect of hydrodynamics (stations 1 – 4) on the theoretical contribution of the sedimentary organic matter sources (obtained from the stable isotopic mixture models, section 2.6) was tested with a two-way ANOVA, using source and station as main factors (after testing assumptions of normality and homoscedasticity). Effects were considered significant at $p < 0.05$.

2.8.4 Organic matter as proxy for C_{org} and N_{total}

Correlation analysis (Pearson's coefficient, r) was performed to test association between organic matter and C_{org}/N_{total}. One-way ANCOVA was used to test for significance of Habitat (main factor) and organic matter (covariate) (effects were

considered significant at $p < 0.05$). Linear regressions were then constructed to predict C_{org} or N_{total} based on ANCOVA results.

2.8.5 Sediment color as proxy for organic matter

Stepwise regression analysis (bidirectional elimination) was performed to select the best model to predict organic matter based on color measurements. The full model included Habitat, L*, a* and b* and all 2-way interactions. Another analysis with log_{10}-transformed organic matter was also done. Addition and removal of predictors was performed and model performance was compared based on AIC (Akaike Information Criterion, Akaike (1974), with the lowest AIC corresponding to the best model).

3 RESULTS

3.1 Vegetation description

All vegetation properties except canopy area were significantly different between *Z. noltei* meadows and *S. maritima* saltmarshes (Table 3.1). Shoot density in *Z. noltei* was higher than in *S. maritima*. Canopy height, above ground biomass and below ground biomass were all lower in *Z.noltei* meadows (Table 3.1).

Table 3.1 - Summary (mean +/- SD) of the structural variables of *Zostera noltei* and *Spartina maritima* averaged across all sampling stations. Results of the 1-way ANOVA (F; Shoot density, Canopy area, Canopy height) or Kruskal-Wallis test ($\chi 2$; AG biomass, BG biomass) are presented, indicating whether the differences across habitats were significant (ns: not significant, *** $p < 0.001$, ** $p < 0.01$, * $p < 0.05$). Superscript lettering represent post-hoc pairwise comparisons indicating differences among the stations. (AG: Above ground, BG: Below ground; DW: dry weight; df: degrees of freedom).

Variable	*S. maritima*	*Z. noltei*	Test (df = 1)
Shoot density (shoots m^{-2})	772.75 ± 269.56	10450.00 ± 4974.75	x2 17.29^{***}
Canopy area (shoots m^{-2})	1.82 ± 0.85	2.68 ± 1.54	F = 2.88^{ns}
Canopy height (cm)	27.83 ± 11.00	8.95 ± 3.92	F = 31.36^{***}
AG biomass (g DW m^{-2})	266.90 ± 154.28	35.39 ± 22.97	x2 = 17.29^{***}
BG biomass (g DW m^{-2})	1093.38 ± 695.34	267.39 ± 133.59	x2 = 11.21^{***}

From the five vegetation properties measured, three varied significantly along the hydrodynamic gradient in both *S. maritima* and *Z. noltei* (Table 3.2). Below-ground biomass and shoot density decreased along the hydrodynamic gradients in both species, being highest at the more exposed station (station 1) and lowest at the most sheltered one (station 4). In *S. maritima* this was accompanied by an increase in canopy height from the two most exposed stations to the two most sheltered. No trend was observed in *Z. noltei* canopy height, despite significant differences amongst stations (Table 3.2). Canopy area and above ground biomass did not display significant differences amongst sampled stations.

Table 3.2 - Summary (mean +/- SD) of the structural variables of *Zostera noltei* and *Spartina maritima* at the four locations sampled, from the closest to the inlet (1) to the furthest (4). Results of the 1-way ANOVA (F; Shoot density, Canopy area, Canopy height) or Kruskal-Wallis test ($\chi 2$; AG biomass, BG biomass) are presented, indicating whether differences across stations were significant (ns: not significant, *** $p < 0.001$, ** $p < 0.01$, * $p < 0.05$). Superscript lettering represent post-hoc pairwise comparisons indicating differences among the stations. (AG: Above ground, BG: Below ground; DW: dry weight; df: degrees of freedom).

Habitat	Variable	Station 1	Station 2	Station 3	Station 4	Test (df = 3)
Zostera noltei	Shoot density (shoots m^{-2})	12733 ± 1939^{ab}	16533 ± 3557^{a}	6400.00 ± 888^{bc}	6133 ± 1738^{c}	$\chi 2 = 9.27$ *
	Canopy area (m^2 m^{-2})	4.13 ± 2.04	3.02 ± 1.61	2.57 ± 1.22	1.00 ± 0.70	F = 3.73 ns
	Canopy height (cm)	12.75 ± 4.03^{a}	6.32 ± 1.56^{ab}	11.14 ± 2.92^{ab}	5.57 ± 1.97^{b}	F = 5.33 *
	AG biomass (g DW m^{-2})	57.03 ± 16.79	32.30 ± 27.47	42.71 ± 5.16	9.52 ± 6.15	$\chi 2 = 6.66$ ns
	BG biomass (g DW m^{-2})	410.63 ± 95.63^{a}	304.99 ± 76.62^{a}	265.71 ± 45.42^{ab}	88.25 ± 6.76^{b}	$\chi 2 = 0.04$ *
Spartina maritima	Shoot density (shoots m^{-2})	1011 ± 53^{a}	1003 ± 161^{a}	561 ± 165^{b}	514 ± 102^{b}	$\chi 2 = 8.44$ *
	Canopy area (m^2 m^{-2})	1.51 ± 0.52	1.53 ± 0.62	2.61 ± 1.57	1.64 ± 0.56	F = 1.23 ns
	Canopy height (cm)	18.48 ± 4.38^{a}	19.57 ± 5.53^{a}	39.38 ± 16.97^{b}	33.89 ± 10.42^{ab}	F = 0.01 *
	AG biomass (g DW m^{-2})	175.14 ± 97.47	193.77 ± 48.79	471.56 ± 169.55	227.13 ± 66.5	$\chi 2 = 0.15$ ns
	BG biomass (g DW m^{-2})	1904.32 ± 430.65^{a}	1427.93 ± 446.35^{ab}	719.62 ± 23.94^{bc}	321.64 ± 129.40^{c}	$\chi 2 = 9.67$ *

3.2 Sedimentary profile description

Cores extracted using 170 cm samplers (ZN and SM) reached sampling depths ranging from 108 to 160 cm (Table 3.3). The core in station CA reached a sampling depth of 56.5 cm. Compaction rates observed ranged from 14.4% to 43.8% (Table 3.3).

Table 3.3 – Core height, sampling depth, compaction correction factor and compaction rates of extracted cores in each location. Core height is the total height of the core, as measured inside the core sampler. Sampling depth refers to the depth reached by the end of each core, after correction due to compaction. Location names abbreviations: CA – *Caulerpa prolifera*; CF – Clam Farm; SM – Spartina maritima; ZN – *Zostera noltei*; 1 – 4 – Station.

Location	Core height (cm)	Sampling depth (cm)	Compaction correction factor (%)	Compaction rate (%)
CA	45	56.5	80.8	19.2
CF	124	145.0	85.5	14.5
SM1	111	134.5	82.5	17.5
SM2	85	108.0	78.7	21.3
SM3	112	160.0	70.0	30.0
SM4	90	160.0	56.3	43.8
ZN1	95	126.7	75.0	25.0
ZN2	98	128.2	76.5	23.6
ZN3	92	140.2	65.6	34.4
ZN4	88	119.8	73.4	26.6

Visual description of the cores is presented in Figure 3.5. The sediment beneath *Caulerpa prolifera* (CA) had two superficial layers of clay, with shells and shell fragments in the first one. These two layers formed the initial 37.1 cm of the core, after which it transitioned to sandy sediment. In the clam farm core (CF), sand constituted most of the core, except for one layer of clay between 26.9 cm and 45.6 cm.

SM and ZN sediment showed a similar trend in how they vary along the hydrodynamic gradient. In general, the clay fraction of the SM and ZN sediment increases as the hydrodynamic energy of the station decreases. In station 1 (SM1), the highest energy environment, there was a superficial clay layer (13.3 cm), before transitioning to sand. Entering the tributary channel, station 2, SM2 showed a similar superficial clay layer, followed by silt from 14 to 66 cm, and another clay layer at the end. SM3 had two clay layers that extended to 101.4 cm of depth, while SM4's clay layers were continuously found until 145.8 cm. ZN1 had an initial clay layer, before transitioning to silt (at 30.7

cm) and then sand (at 61.3 cm). ZN2 has a shallower superficial layer than ZN1, but transitions into silt and then again into clay, showing its first sandy layer at a depth of 85 cm. ZN3 was constituted of clay sediment in its entirety (140.2 cm) and ZN4 until 85.8 cm, after which it transitions to sandy sediment.

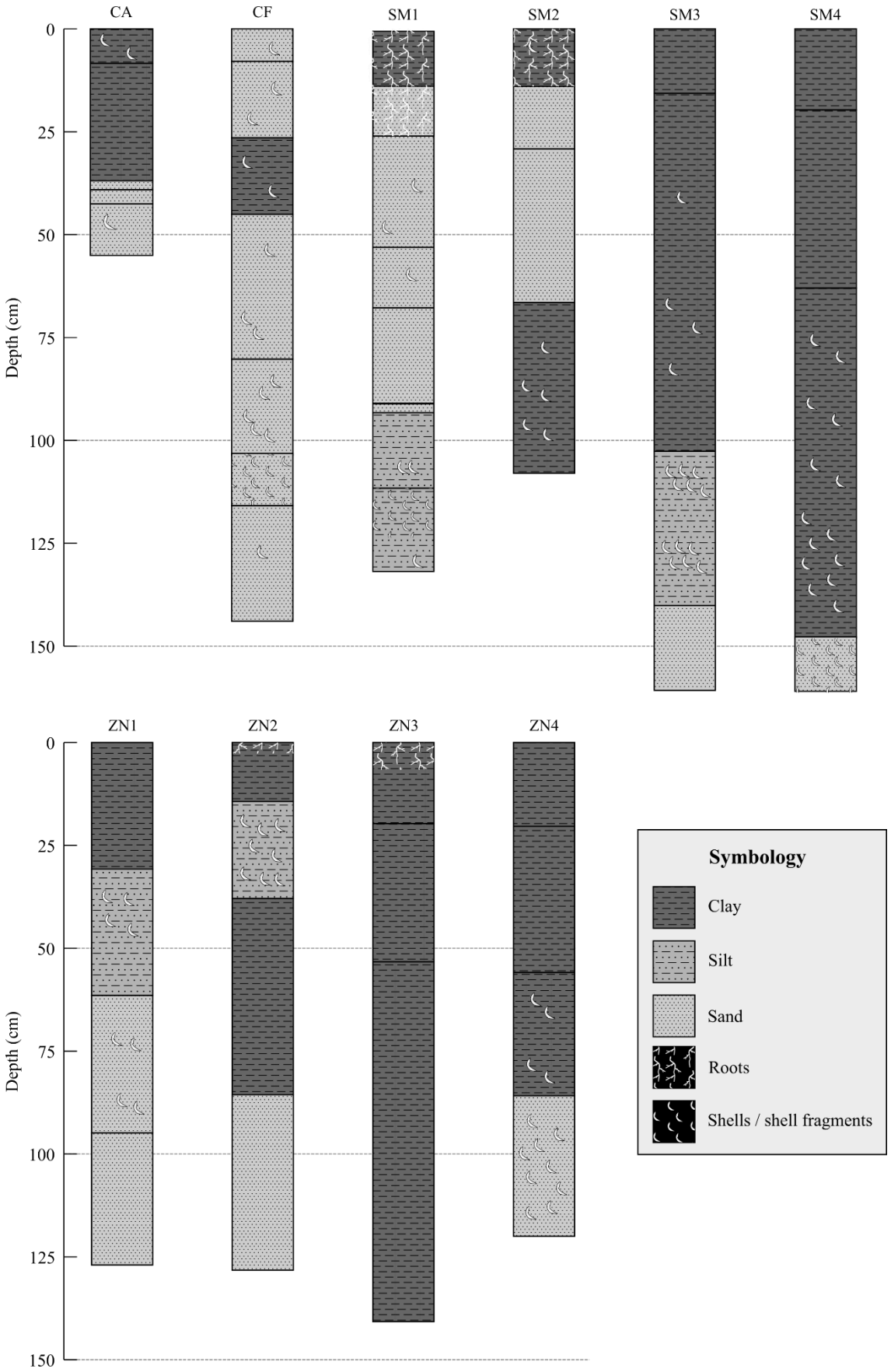

Figure 3.5- Visual descriptions of the sediment cores and symbology used. Location names abbreviations: CA – *Caulerpa prolifera*; CF – Clam Farm; SM – *Sparina maritima*; ZN – *Zostera noltei*; 1 – 4 – Station.

3.3 Sedimentary C_{org} and N_{total}: variation along hydrodynamic gradient

The median values for *Z. noltei* and *S. maritima* sedimentary C_{org} contents, 1.31% and 1.11%, respectively were not significantly different from each other (Figure 3.6a). They were, however, significantly higher than both *C. prolifera*'s and the clam farm, which had median values of 0.50% and 0.23%, respectively. The same trend was observed for N_{total} (Figure 3.6b), where the median values for *Z. noltei* and *S. maritima* were significantly higher than for *C. prolifera* and clam farm.

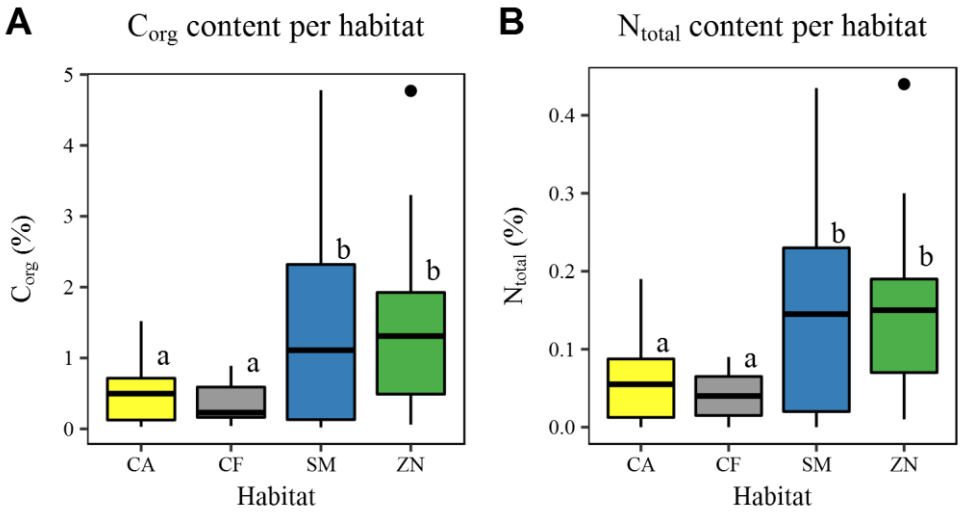

Figure 3.6 - Sedimentary organic carbon (A) and total nitrogen (B) content in sampled habitats. Boxplots components from middle out: thick line inside the boxes represents the median; boxes extend from 25th to 75th percent quantile; whiskers extend up to 1.5 x IQR; values outside of the whisker's range are considered outliers and plotted as dots. Lettering above the boxes represents homogenous groups ($p < 0.05$, Dunn's test). Location names abbreviations: CA – Caulerpa prolifera; CF – Clam Farm; SM – Sparina maritima; ZN – *Zostera noltei*; 1 – 4 – Station.

Considering a sediment depth of 100 cm, the amount of C_{org} per area of habitat in SM and ZN was not significantly different (0.80 ± 0.36 and 0.81 ± 0.26 g C_{org} cm^{-2}, respectively) (Figure 3.7). N_{total} storage did not differ either for SM and ZN (0.082 ± 0.040 and 0.087 ± 0.019 g N_{total} cm^{-2}, respectively). Stocks of C_{org} (0.36 g C_{org} cm^{-2}) and N_{total} (0.044 g N_{total} cm^{-2}) in the clam farm were lower than the two vegetated intertidal habitats (Figure 3.7).

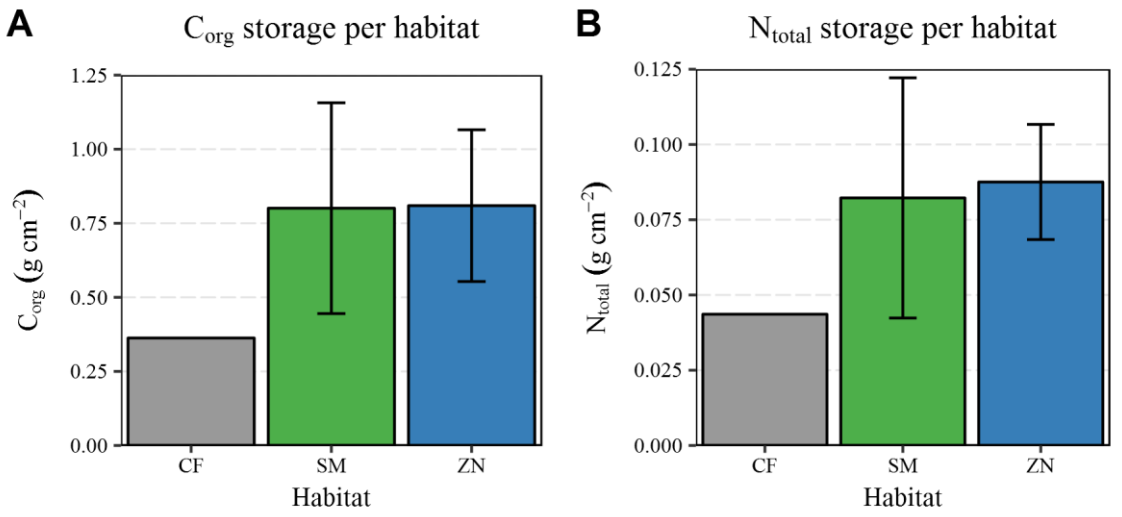

Figure 3.7 – Organic carbon (A) and total nitrogen (B) storage per area of habitat. Values were calculated from the sediment surface to a depth of 100 cm. ZN and SM are averaged over the 4 sampled locations. Location names abbreviations: CF – Clam Farm; SM – Sparina maritima; ZN – *Zostera noltei*.

In general, C_{org} decreased over sediment depth (Figure 3.8). In *Z. noltei* and *S. maritima* sediment, this decrease was more accentuated at shallow depths and then stabilized (Figure 3.8).

The clam farm sediment showed less variation in C_{org} content. Throughout the profile, values remained below 0.33%, except for sediment between 19.9 and 43.3 cm, where values up to 0.89% were measured (Figure 3.8). This depth partially coincides with the change from sand to clay (Figure 3.5, Annex 2).

The depth variation of C_{org} in *S. maritima* stations 1 and 2 was similar, ranging from 3.1% to 4.8% for the first 10 cm, whereas in stations 3 and 4 it ranged from 2.2% to 2.9%, also in the first 10 cm. A sharp decline is then seen on stations 1 and 2, to values from 0.02% to 0.37%, from 15 to 65 cm of depth, coincident with the change from clayey to sandy sediment (Annex 2). After 65 cm, a strong increase was observed, more accentuated and coincident with a return to clayey sediment in SM2 (Annex 2). Stations 3 and 4 showed a decrease in C_{org} content after the initial 10 cm until the end of the cores, when $\%C_{org}$ reached a minimum of 0.09% and 0.58%, respectively. Station 4 also showed a relevant increase from 1.3% at 80 cm to 2.7% at 87.1 cm. At depths higher than 125 cm, the C_{org} within *S. maritima* sediment tended to approach 0% (Figure 3.8).

The depth variation of C_{org} in *Z. noltei* showed very similar trends across stations, ranging from 0.5% to 1.57% for the first 12 cm in stations 1 and 2. C_{org} in stations 3 and

4 was high in the top 12 cm, ranging from 1.53% to 2.38%. After this depth (12 cm), the organic carbon content remains stable until 50 to 57 cm of depth. Afterwards, C_{org} content in station 1 and 3 began a gradual decrease until the end of the core. Station 2 had an increase in organic carbon content to 1.34% at 58.9 cm, after which a decrease was observed until the end of the core. Station 3, however, showed a constant increase in C_{org} content after 57 cm, reaching a peak for the whole depth range of 4.77% C_{org} at 138.7cm. The pattern seen amongst levels was similar to the one observed in SM, with station pairs 1-2 and 3-4 showing similar trends and values, being values higher at stations 3-4 (lower hydrodynamics) than at stations 1-2 (higher hydrodynamics) (Figure 3.8).

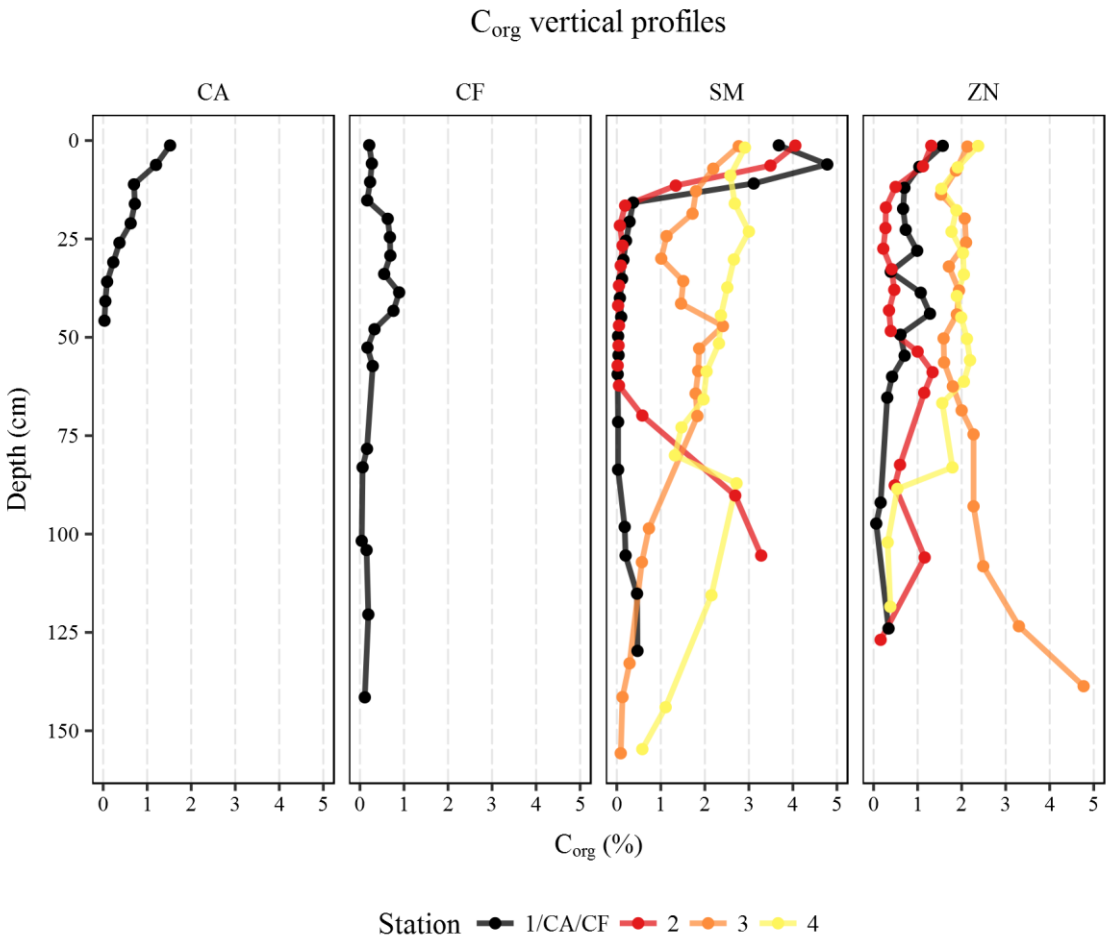

Figure 3.8 – Vertical profiles of organic carbon content for all sampled cores. Location names abbreviations: CA – *Caulerpa prolifera*; CF – Clam Farm; SM – Spartina maritima; ZN – *Zostera noltei*; 1 – 4 – Station.

The amount of C_{org} stored per area, at a sediment depth of 100 cm, increased as the hydrodynamic energy of the station decreased (Figure 3.9). Sediment at stations ZN2, ZN3 and ZN4 contained 1.30, 1.83 and 2.08 times more C_{org} per area than ZN1. The differences found in the *S. maritima* habitat were even more accentuated: 2.38, 3.30 and 3.44 when comparing SM2, SM3 and SM4 to SM1. Clam farm contained 0.36 g C_{org} cm^{-2} (Figure 3.9).

N_{total} storage once again followed the same pattern as C_{org}. In *S. maritima* sediment N_{total} storage increased from 0.03 g N_{tota} cm^{-2} in the most exposed station (1) to 0.11 g C_{org} cm^{-2} at the most sheltered (4). In *Z. noltei* meadows' sediment, N_{total} storage increased from 0.07 g N_{tota} cm^{-2} to 0.11 g N_{tota} cm^{-2}, from station 1 to 4 (Figure 3.9).

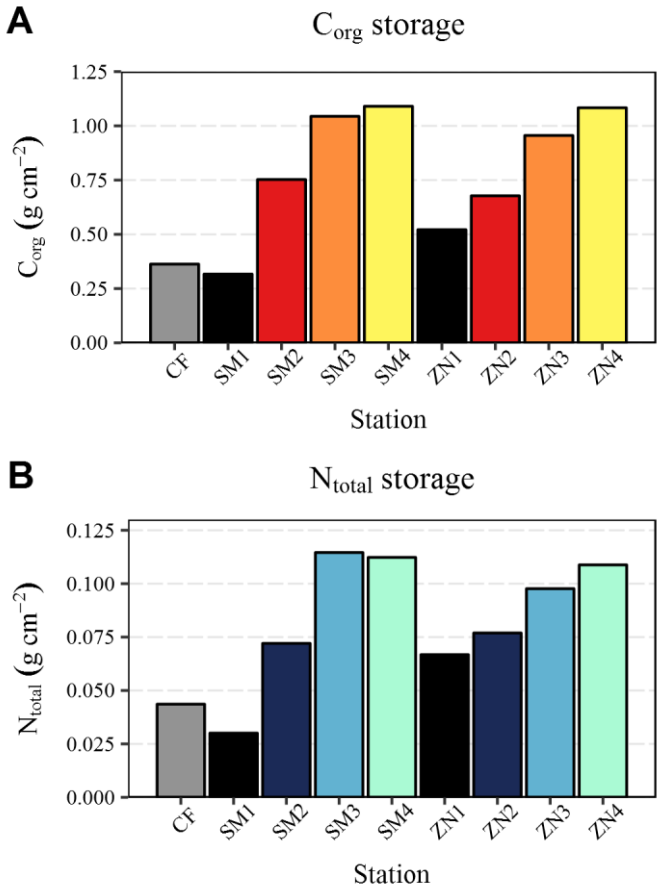

Figure 3.9 - Sedimentary organic carbon (A) and total nitrogen (B) storage per surface area at each location. Values were calculated from the sediment surface to a depth of 100 cm. Location names abbreviations: CF – Clam Farm; SM – Sparina maritima; ZN – *Zostera noltei*; 1 – 4 – Station.

Step-wise regression indicated that the best model to describe C_{org} content includes the predictors Station, log_{10}-transformed Depth, plus interaction Station:log_{10} Depth (AIC = -42.82, R^2 = 0.43, df = 128; Table 3.4). Regressions obtained show that C_{org} decrease over depth is lower in stations with low hydrodynamics (stations 3 and 4) than in more exposed stations (stations 1 and 2) (Figure 3.10).

Mean C_{org} content values were significantly higher in the two most sheltered stations (stations 3 and 4) than in exposed stations (stations 1 and 2). No significant differences were found between average C_{org} contents of stations 1 and 2 or between stations 3 and 4 (Figure 3.11).

Table 3.4 – Result of changes to predictors to the best model for estimating organic carbon, selected by stepwise regression. Changes consist of adding (+), removing (-) or leaving the model as is (None, i.e. results for best selected model) (df = degrees of freedom, SS = Sum of squares, RSS = residual sum of squares, AIC = Akaike information criterion).

	Non-transformed depth				**Log10-transformed depth**			
Change	**df**	**SS**	**RSS**	**AIC**	**df**	**SS**	**RSS**	**AIC**
None			99.8	-26.0			88.3	-42.8
+Habitat	1	0.2	99.7	-24.3	1	0.1	88.2	-40.9
- Level:Depth	3	6.1	106.0	-24.0	3	5.9	94.2	-40.0

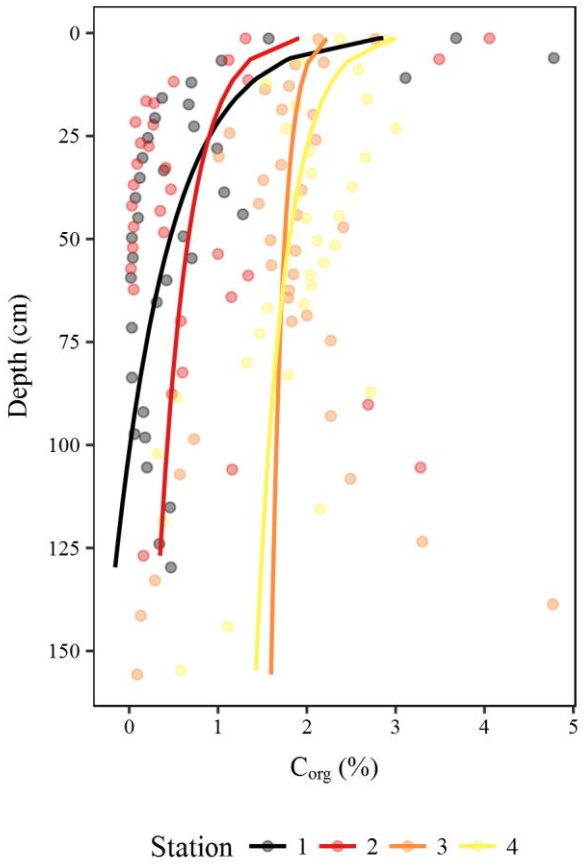

Figure 3.10 - Visualization of the full model to estimate $\%C_{org}$ using station, log_{10}-transformed Depth and respective interaction as predictors. Lines represent values estimated by linear model, points represent data used to construct the model. Location names abbreviations: SM – Spartina maritima; ZN – *Zostera noltei*; 1 – 4 – Station.

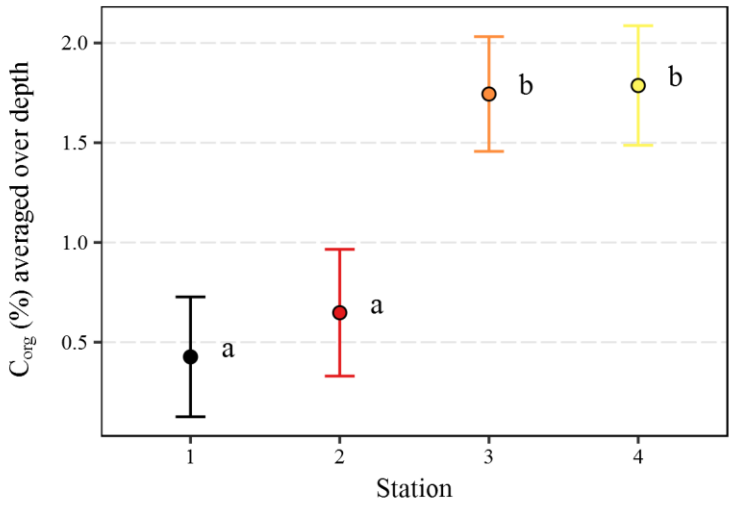

Figure 3.11 – Marginal mean ± 95% confidence interval for sedimentary organic carbon ($\%C_{org}$) in each sampling station (station 1 being the one closest to the inlet and more exposed to waves and tidal currents, and station 4 being the furthest to the inlet and the most shelter). Lettering adjacent to the points represents homogenous groups ($p < 0.05$, Tukey's HSD).

3.4 Organic matter provenance

The great majority of the samples fell within the limits established by the isotopic values of the organic matter sources (Figure 3.12), suggesting that the sedimentary OM could be purely a mixture of the sampled sources, without major influence of other sources. No clear separation or pattern was observed among stations, i.e. along the hydrodynamical gradient.

Isotopic signatures of all sources were different, both in $\delta^{13}C$ and $\delta^{15}N$, except for *Z. noltei* and *S. maritima*. These two sources had significantly different $\delta^{13}C$ ($df = 1$; $F = 219.24$, $p < 0.001$), but not $\delta^{15}N$ ($df = 1$; $F = 1.94$, $p = 0.17$). As such, contributions of these sources might not be distinguishable and sources were combined *a-posteriori*, as recommended by the model authors (Parnell et al., 2013).

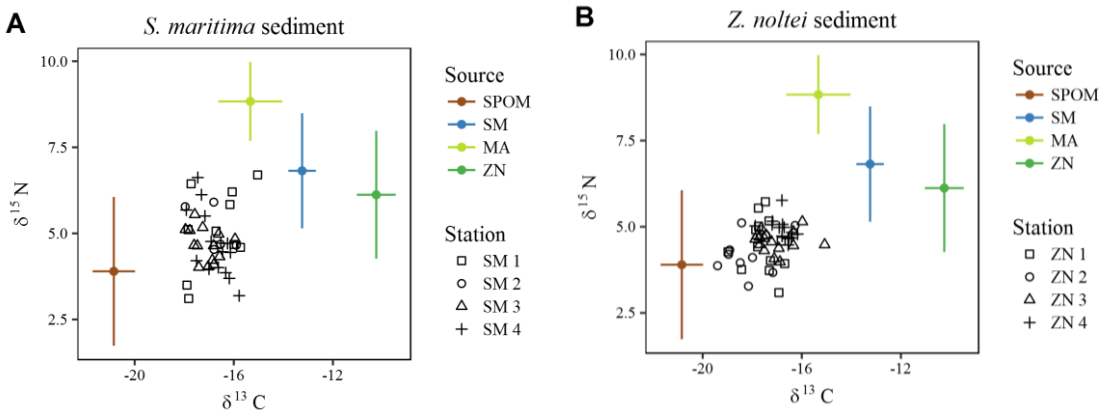

Figure 3.12 – Iso-space plots of isotopic signatures of sediment samples and selected organic matter sources for (A) *Spartina maritima* and (B) *Zostera noltei* sediments. SPOM – Suspended particulate organic matter; MA – macroalgae; SM –*Spartina maritima*; ZN – *Zostera noltei*.

Suspended particulate organic matter (SPOM) and *S. maritima* plus *Z. noltei* organic matter (ZN+SM) were the major contributors (Figure 3.13). In *S. maritima* sediment, SPOM contributed between 49 and 55% of the total organic matter and ZN+SM contributed from 36 to 39%, while macroalgae (MA) contributed from 7 to 11%. In sediment from the *Z. noltei* habitat, the contribution of SPOM ranged from 50 to 66%. ZN+SM contributed from 24 to 36% and MA only 7 to 10% (Figure 3.13).

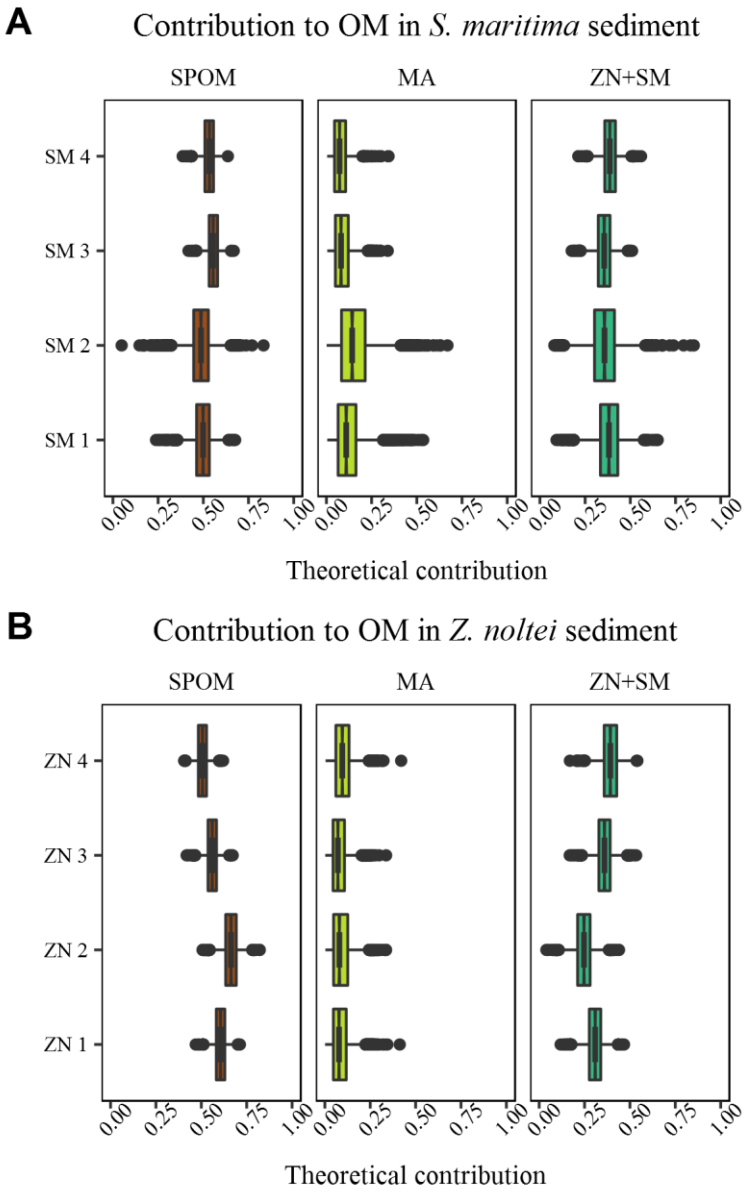

Figure 3.13 – Organic matter source contribution for (A) *Sparina maritima* sediment and (B) *Zostera noltei* sediment. Sources name abbreviation: SPOM = Suspended particulate organic matter; MA = macroalgae; SM = *Spartina maritima*; ZN = *Zostera noltei*.

In *Z. noltei* sediment, the contribution of ZN+SM appeared to increase along the hydrodynamic gradient, while SPOM contribution decreased, which is reflected in the interaction term of ANOVA (Table 3.5). No significant differences were found in the contribution to sedimentary organic matter along the hydrodynamic gradient in *S. maritima* sediment (Table 3.5, Figure 3.13).

Table 3.5 – Two-way ANOVA results for effect of source and station on theoretical contribution to sedimentary organic matter (SS = Sum of squares, df = degrees of freedom, F = F statistic, p = p-value).

Habitat	Predictor	SS	df	F	p
SM	Source	222.80	2	24523	< 0.001
	Station	0.00	1	0.85	0.36
	Source:Station	0.01	2	0.79	0.45
ZN	Source	322.20	2	37167	< 0.001
	Station	0.00	1	0.01	0.93
	Source:Station	0.03	2	3.8	< 0.02

3.5 Proxies for C_{org}, N_{total} and OM

3.5.1 OM content as a proxy for C_{org} and N_{total}

The relation between organic matter content, C_{org} and N_{total} contents was significant and did not significantly differ across habitats (Table 3.6). Relations between organic matter content and elemental contents from data of all habitats obtained r^2 values of 0.92 (Figure 3.14). This indicates that accurate C_{org} and N_{total} content estimates can be obtained through organic matter content, in the Ria Formosa.

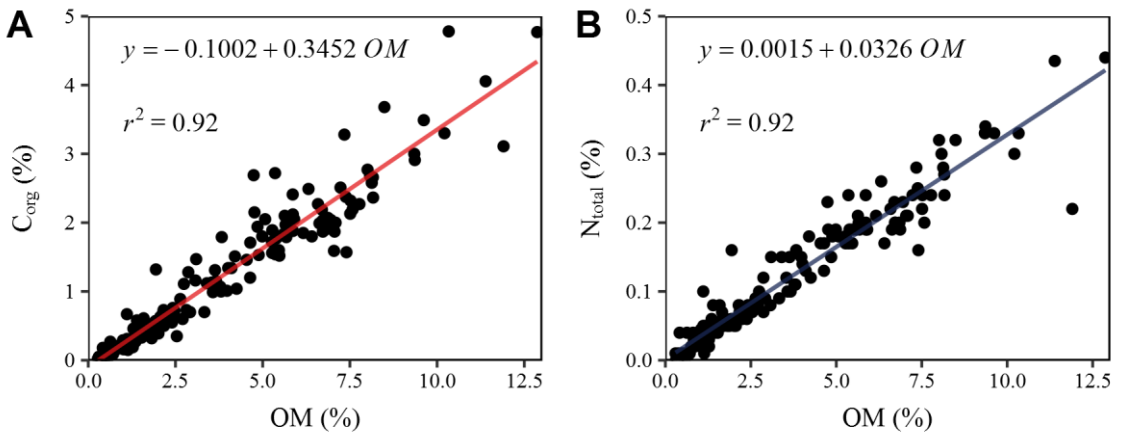

Figure 3.14 - Linear relationships between organic matter content (OM), organic carbon content (C_{org}, A) and total nitrogen content (N_{total}, B), in sediment of *Spartina maritima*, *Zostera noltei*, *Caulerpa prolifera* and clam farm stations.

Table 3.6 – One-way ANCOVA to test the effect of organic matter content (OM) and Habitat on organic carbon content (C_{org}) and total nitrogen content (N_{tota}). (SS = Sum of squares, df = degrees of freedom, F = F statistic, p = p-value)

Dependent variable	Predictor	SS	df	F	p
C_{org}	OM	2.27	1	28.21	< 0.001
	Habitat	0.08	3	0.33	0.80
	OM:Habitat	0.21	3	0.86	0.46
N_{total}	OM	0.03	1	46.13	< 0.001
	Habitat	< 0.01	3	1.24	0.30
	OM:Habitat	< 0.01	3	1.85	0.14

3.5.2 Sediment color as proxy for OM

Negative correlations were found between organic matter content in the sediment and both lightness (L*, r = -0.21, $p < 0.05$) and green-red (a*, r = -0.28, $p < 0.05$). The dimension blue-yellow (b*) was positively correlated (r = 0.45, $p < 0.05$). Step-wise regression indicated that the best model to predict organic matter content includes the predictors Habitat, L*, b* and L*:Habitat interaction (AIC = 306.84, $R^2 = 0.30$, df = 160; Table 3.7). Applying a $\log_{10}$ transformation to organic matter content values increased the performance of the model (AIC = -355.48, $R^2 = 0.43$, df = 160, Table 3.7). Therefore, final models to predict %OM based on sediment color included the predictors the L* and b* and they were specific for each habitat (to include the interaction) (Table 3.8).

Table 3.7 – Result of changes to predictors to the best models selected by stepwise regression. Changes consist of adding (+), removing (-) or leaving the model as is (None, i.e. results for best selected model) (df = degrees of freedom, SS = Sum of squares, RSS = residual sum of squares, AIC = Akaike information criterion).

	Non-transformed %OM				Log10-transformed %OM			
Change	**df**	**SS**	**RSS**	**AIC**	**df**	**SS**	**RSS**	**AIC**
None			934.5	304.9			15.8	-372.3
+ L*:b*	1	2.0	932.5	306.5	1	< 0.1	15.8	-370.3
+ a*	1	0.7	933.8	306.7	1	< 0.1	15.8	-370.3
- Habitat:L*	3	46.0	980.6	306.8	3	2.3	18.1	-355.5
+Habitat:b*	3	16.3	918.2	307.9	3	0.2	15.6	-368.6
- b*	1	141.6	1076.1	326.3	1	4.0	19.8	-337.1

Table 3.8 – Equations to predict organic matter content in sediment obtained by the best model selected by stepwise regression (R^2 = 0.43, df = 160).

Habitat	Equation
CA	$Log_{10}(OM) = 1.6459 + 0.0258\ b^* - 0.0612\ L^*$
CF	$Log_{10}(OM) = 0.2578 + 0.0258\ b^* - 0.0013\ L^*$
SM	$Log_{10}(OM) = 1.5802 + 0.0258\ b^* - 0.0350\ L^*$
ZN	$Log_{10}(OM) = 0.8021 + 0.0258\ b^* - 0.0094\ L^*$

The model achieved an R^2 of 0.43, indicating that accuracy of estimates is not very high. Evaluation of fitted vs predicted values per habitat showed that the model tends to overestimate the sedimentary OM at low organic matter contents and underestimate it at high organic matter contents. This effect is most pronounced in *Z. noltei* samples (Figure 3.15).

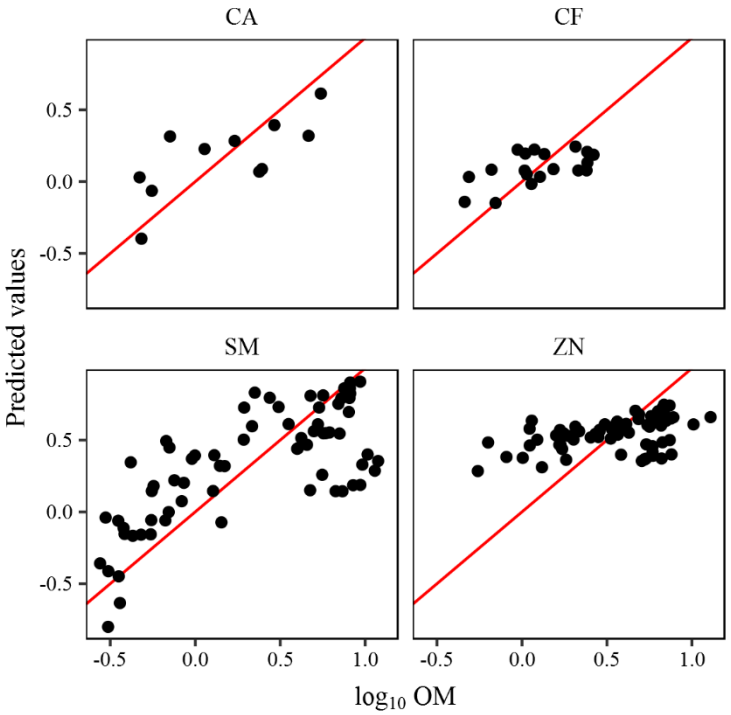

Figure 3.15 – Actual and predicted organic matter contents (log_{10} transformed) in the sampled habitats. Predictions were estimated using a model with Habitat, L* and b* as predictors (R^2 = 0.43, df = 160). Red line corresponds to the point where predicted values equal actual values (1:1). Location names abbreviations: CA – *Caulerpa prolifera*; CF – Clam Farm; SM – *Spartina maritima*; ZN – *Zostera noltei*.

4 DISCUSSION

4.1 Sedimentary profile description

In *Z. noltei* and *S. maritima* sediment, the fraction of the core classified as clay/silt increased from station 1 to station 4. This trend supports the existence of a hydrodynamic gradient along the ZN and SM stations previously reported (Núñez, 2015), since low size particles are mostly deposited in areas of low hydrodynamic energy regimes (Shi, 2009). This spatial hydrodynamic gradient is in line with patterns observed in many documented estuaries and lagoons, where a fining of sediments is found as we move from the mouth to the head of the estuary (Bianchi, 2007).

The composition of the clam farm sediment (mainly sand) is expected, since areas used for clam cultivation are kept clean of vegetation and regularly receive anthropogenic sand deposits to help reduce vegetation growth (Cunha et al., 2005). Only one layer of small sediment size was found, between 26.9 cm and 45.6 cm, and it could correspond to sediment accumulated during the 40 years (1960 to 2000) during which exploitation of this location for bivalve production was stopped, before another layer of sand was deposited.

4.2 Organic carbon storage

Organic carbon storage capacity per area in coastal vegetated habitats (*Z. noltei* and *S. maritima*) was approximately twice as high as in the clam farm. This is likely due to several factors, including: a) presence of vegetation promoting higher deposition rates and stabilization of deposited sediment (Hendriks et al., 2008); b) differences in grain size: the presence of vegetation promoted deposition of thin sediment that increases anoxia conditions in the sediment and reduces decomposition rates (Cebrian, 1999); c) organic matter produced in-situ: C_{org} incorporated in OM produced in these areas can be directly sequestered to the sediment , while the clam farm relies mostly on allochthonous OM. Guimarães et al., 2012 estimated that, according to the current Ria Formosa management plan, approximately 63% of the *Z. noltei* meadows in the Ria were in areas where both clam farming and digging were allowed without significant restrictions. While conversion of seagrass meadows to clam farming areas might not remove all C_{org} stocks already in place (specially the OM sequestered in deep sediment layers) (Marbà et al.,

2015), the vegetation removal plus the human disturbance of the superficial sediment (digging) is likely to lead to a significant erosion of the superficial stocks and cause a reduction of future carbon sequestration capacity of these areas (Marbà et al., 2015).

In *Z. noltei* and *S. maritima* sediment, superficial C_{org} contents were high, followed by a short and rapid decrease in C_{org} and then a slower decrease. This indicates a continuous decomposition of the organic matter trapped in the sediment along time, with an initial period of quicker degradation. This period corresponds to the degradation of the more labile organic matter, in combination with aerobic conditions of the superficial sediments. The high C_{org} contents in stations SM2 and ZN3 indicates that to C_{org} storage estimations might require deeper sedimentary column sampling in some locations.

Estimated C_{org} storage in the top meter of *S. maritima* and *Z. noltei* areas in the Ria Formosa fell below global average values reported for similar habitats (Duarte et al., 2013b; Fourqurean et al., 2012). This suggests that usage of global means to estimate organic carbon stocks will lead to overestimations. This was expected for *Z. meadows*, as the carbon burial capacity of this species is lower than many of the commonly reported seagrass species (Duarte et al., 2013a). However, it fell above ranges reported for *Z. marina* and several Australian species (Dahl et al., 2016a; Lavery et al., 2013), reinforcing the idea that *Z. noltei* is a significant species for carbon sequestration.

A large impact of the hydrodynamic gradient present along sampling stations was found, with sheltered stations holding up to 3.44 times more organic carbon than the most exposed station. The changes in hydrodynamics can cause difference carbon storage rates due to a combination of: 1) higher organic matter deposition rates and stability (less resuspension) at lower hydrodynamic energies (Marbà et al., 2015; Serrano et al., 2016a); b) higher sedimentation rates at lower hydrodynamic regimes, leading to a higher organic matter burial rate (Bianchi, 2007); c) different oxygenation levels caused by differences in sediment size. The sediment profile description showed an overall increase in thin sediments as the station level increased, which promote the formation of anoxic conditions and can lead to reduced degradation rates sediments in the more sheltered stations (Ricart et al., 2015). The similarities in carbon and nitrogen stocks between pairs of stations (1-2 and 3-4) might be explained by the hydrodynamic regime not being linearly related to distance to the inlet (factor used to determine sampling stations).

4.3 Organic matter provenance

Previous studies found no significant changes in $\delta 13C_{org}$ and $\delta 15N$ due decomposition of *Z. noltei* leaves (Machás et al., 2006), but the effect has been considered strong enough to be incorporated in some mixing models, with a diagenesis correction term (Greiner et al., 2016). Estimations of the long-term impacts of anaerobic decomposition on the signature of our organic matter sources were not available, but exclusion of samples with correlation between diagenesis and elemental signature changes should help reduce the error induced by this process.

The organic matter source contributions indicate that suspended particulate organic matter is the largest source of organic matter in *Z. noltei* and *S. maritima* sediment. Primary production in the habitats (*Z. noltei* plus *S. maritima* biomass) is the second largest, with a much smaller contribution from macroalgae.

Differences in habitat location along the zonation profile (*Z. noltei* meadows are subjected to longer periods underwater and therefore longer exposure to the effects of hydrodynamics, Guimarães et al., 2012), in addition higher sedimentation rates in *Z. noltei* (Lahuna, 2017) and higher standing biomasses in *S. maritima* suggested that *Z. noltei* would have higher contribution from SPOM deposition, but that was not observed. In *Z. noltei*, *c*ontribution of *Z. noltei* plus *S. maritima* tissue in was higher in more sheltered stations. This phenomenon might be explained by the differences in exposure to hydrodynamic effects, with more exposed stations exporting a larger fraction of primary productivity (Dahl et al., 2016a; Röhr et al., 2016). *Z. noltei* tissue is also know to float when detached from the sediment, promoting exportation of primary productivity and enhancing the effect of hydrodynamics (Tyler-Walters, 2005).

4.4 Proxies for C_{org}, N_{total} and OM

Linear relationships between organic matter content and elemental contents are a good proxy to estimate the latter two parameters in the sediment of all sampled habitats. Using the determined equations allows future works to estimate with a high confidence the carbon or nitrogen contents in sediment in the Ria Formosa without directly analyzing elemental contents, which is advantageous due to the simplicity and inexpensiveness of organic matter measurements through loss on ignition.

Sediment color can be used to estimate organic matter contents in the sediment. Sediment color can used as a rough and quick estimator of organic matter contents, avoiding the relatively long (2 days) process of a loss on ignition methodology. Previous studies suggest that color in marine sediment is mostly determined by mineralogy, diagenesis and oxidation/reduction reactions (Bianchi, 2007; Giosan et al., 2002), with significant changes between color and sediment properties across and temporal scales (Balsam et al., 1999). This suggests that to improve predictions of organic matter content based on sediment color, many sediment properties need to be measured. This methodology could be adapted to be used on the field, allowing rough estimations of organic matter content without transporting samples and laboratory analysis. However, if very accurate organic matter measurements are needed (e.g. for scientific research), traditional laboratory methods are preferred.

5 CONCLUSIONS

- The sedimentary profiles in *Z. noltei* and *S. maritima* stations supported the previous findings regarding the hydrodynamic gradient along the stations, while supporting the idea that clam farm sediment is comprised mostly of sediment.

- Differences in carbon storage capacity of the habitats were found, with higher carbon storage in vegetated intertidal habitats (*Z. noltei* and *S. maritima*) than in a clam farm. No differences between the two vegetated habitats were found, but there were indications that *Z. noltei* stocks extend up to higher depths than those of *S. maritima*. Further sampling, extending to higher depths, is required to test this hypothesis.

- Differences in C_{org} storage along the hydrodynamic gradient were also found, with sheltered stations (3-4) storing larger amounts of sedimentary organic carbon than the exposed stations (1-2). Suspended particulate organic matter and autochthonous organic matter were the major contributors to sedimentary organic matter, with similar contributions, but no significant trend was observed in those contributions along the hydrodynamical gradient.

- Organic matter is a very accurate proxy to estimate both C_{org} and N_{total}. Sediment color can be used to estimate for organic matter, but it is not equally useful in all sampled habitats and leaves a high value of variability unexplained, likely due to untested differences in the color of sediment particles.

6 BIBLIOGRAPHY

Adobe Systems Incorporated. (2000). Color models: CIELAB. Retrieved from http://dba.med.sc.edu/price/irf/Adobe_tg/models/cielab.html

Akaike, H. (1974). A new look at the statistical model identification. *IEEE Transactions on Automatic Control*, *19*(6), 716–723. https://doi.org/10.1109/TAC.1974.1100705

Arnaud-Fassetta, G., Bertrand, F., Costa, S. & Davidson, R. (2006). The western lagoon marshes of the Ria Formosa (Southern Portugal): Sediment-vegetation dynamics, long-term to short-term changes and perspective. *Continental Shelf Research*, *26*(3), 363–384. https://doi.org/10.1016/j.csr.2005.12.008

Avnimelech, Y., Ritvo, G., Meijer, L. E. & Kochba, M. (2001). Water content, organic carbon and dry bulk density in flooded sediments. *Aquacultural Engineering*, *25*(1), 25–33. https://doi.org/10.1016/S0144-8609(01)00068-1

Bach, S., Thayer, G. & LaCroix, M. (1986). Export of detritus from eelgrass (Zostera marina) beds near Beaufort, North Carolina, USA. *Marine Ecology Progress Series*, *28*(1967), 265–278. https://doi.org/10.3354/meps028265

Balsam, W. L., Deaton, B. C. & Damuth, J. E. (1999). Evaluating optical lightness as a proxy for carbonate content in marine sediment cores. *Marine Geology*, *161*(2–4), 141–153. https://doi.org/10.1016/S0025-3227(99)00037-7

Bianchi, T. S. (2007). *Biogeochemistry of Estuaries*. New York: Oxford University Press.

Bigham, J. M., Ciolkosz, E. J. & Schwertmann, U. (1993). Relations Between Iron Oxides, Soil Color, and Soil Formation. https://doi.org/10.2136/sssaspecpub31.c4

Cebrian, J. (1999). Patterns in the Fate of Production in Plant Communities. *The American Naturalist*, *154*(4), 449–468. https://doi.org/10.1086/303244

Ceia, F. R. (2009). Vulnerabilidade das Ilhas-Barreira e Dinâmica da Ria Formosa na Óptica da Gestão. *Revista de Gestão Costeira Integrada*, *9*(1), 57–77. https://doi.org/10.5894/rgci159

Costanza, R., de Groot, R., Sutton, P., van der Ploeg, S., Anderson, S. J., Kubiszewski, I., Farber, S. & Turner, R. K. (2014). Changes in the global value of ecosystem services. *Global Environmental Change*, *26*(1), 152–158. https://doi.org/10.1016/j.gloenvcha.2014.04.002

Cunha, a. H., Santos, R. P., Gaspar, a. P. & Bairros, M. F. (2005). Seagrass landscape-scale changes in response to disturbance created by the dynamics of barrier-islands: A case study from Ria Formosa (Southern Portugal). *Estuarine, Coastal and Shelf Science*, *64*, 636–644. https://doi.org/10.1016/j.ecss.2005.03.018

Dahl, M., Deyanova, D., Gütschow, S., Asplund, M. E., Lyimo, L. D., Karamfilov, V., Santos, R., Björk, M. & Gullström, M. (2016a). Sediment Properties as Important Predictors of Carbon Storage in Zostera marina Meadows: A Comparison of Four European Areas. *PLOS ONE*, *11*(12). https://doi.org/10.1371/journal.pone.0167493

Dahl, M., Deyanova, D., Lyimo, L. D., Näslund, J., Samuelsson, G. S., Mtolera, M. S., Björk, M. & Gullström, M. (2016b). Effects of shading and simulated grazing on carbon sequestration in a tropical seagrass meadow. *Journal of Ecology*, *104*(3), 654–664. https://doi.org/10.1111/1365-2745.12564

Duarte, C. M., Kennedy, H., Marbà, N. & Hendriks, I. (2013a). Assessing the capacity of seagrass meadows for carbon burial: Current limitations and future strategies. *Ocean and Coastal Management*, *83*. https://doi.org/10.1016/j.ocecoaman.2011.09.001

Duarte, C. M., Losada, I. J., Hendriks, I. E., Mazarrasa, I. & Marbà, N. (2013b). The role of coastal plant communities for climate change mitigation and adaptation. *Nature Climate Change*, *3*(11), 961–968. https://doi.org/10.1038/nclimate1970

Duarte, C. M., Middelburg, J. J. & Caraco, N. (2004). Major role of marine vegetation on the oceanic carbon cycle. *Biogeosciences Discussions*, *1*(1), 659–679. https://doi.org/10.5194/bgd-1-659-2004

Ekstrøm, C. T. (2017). MESS: Miscellaneous Esoteric Statistical Scripts. Retrieved from https://cran.r-project.org/package=MESS

Fourqurean, J. W., Duarte, C. M., Kennedy, H., Marbà, N., Holmer, M., Mateo, M. A., Apostolaki, E. T., Kendrick, G. a., Krause-Jensen, D., McGlathery, K. J. & Serrano, O. (2012). Seagrass ecosystems as a globally significant carbon stock. *Nature Geoscience*, *5*(7), 505–509. https://doi.org/10.1038/ngeo1477

Friend, P. L., Ciavola, P., Cappucci, S. & Santos, R. (2003). Bio-dependent bed parameters as a proxy tool for sediment stability in mixed habitat intertidal areas. *Continental Shelf Research*, *23*(17–19), 1899–1917. https://doi.org/10.1016/j.csr.2002.12.001

Gacia, E. & Duarte, C. M. (2001). Sediment Retention by a Mediterranean Posidonia oceanica Meadow: The Balance between Deposition and Resuspension. *Estuarine, Coastal and Shelf Science*, *52*(4), 505–514. https://doi.org/10.1006/ecss.2000.0753

Giosan, L., Flood, R. D., Grützner, J. & Mudie, P. (2002). Paleoceanographic significance of sediment color on western North Atlantic Drifts: II. Late Pliocene-Pleistocene sedimentation. *Marine Geology*, *189*(1–2), 43–61. https://doi.org/10.1016/S0025-3227(02)00322-5

Glew, J. R., Smol, J. P. & Last, W. M. (2001). Sediment Core Collection and Extrusion. In *Tracking Environmental Change Using Lake Sediments* (Vol. 1, pp. 73–105). Dordrecht: Kluwer Academic Publishers. https://doi.org/10.1007/0-306-47669-X_5

Greiner, J., Wilkinson, G., McGlathery, K. & Emery, K. (2016). Sources of sediment carbon sequestered in restored seagrass meadows. *Marine Ecology Progress Series*, *551*, 95–105. https://doi.org/10.3354/meps11722

Guimarães, M. H. M. E., Cunha, A. H., Nzinga, R. L. & Marques, J. F. (2012). The distribution of seagrass (Zostera noltii) in the Ria Formosa lagoon system and the implications of clam farming on its conservation. *Journal for Nature Conservation*, *20*(1), 30–40. https://doi.org/10.1016/j.jnc.2011.07.005

Harrison, P. G. (1989). Detrital processing in seagrass systems: A review of factors affecting decay rates, remineralization and detritivory. *Aquatic Botany*, *35*(3–4), 263–288. https://doi.org/10.1016/0304-3770(89)90002-8

Heiri, O., Lotter, A. F. & Lemcke, G. (2001). Loss on ignition as a method for estimating organic and carbonate content in sediments: reproducibility and comparability of results. *Journal of Paleolimnology*, *25*(1), 101–110. https://doi.org/10.1023/A:1008119611481

Hendriks, I., Sintes, T., Bouma, T. & Duarte, C. (2008). Experimental assessment and modeling evaluation of the effects of the seagrass Posidonia oceanica on flow and particle trapping. *Marine Ecology Progress Series*, *356*, 163–173. https://doi.org/10.3354/meps07316

Hopkins, J. B. & Ferguson, J. M. (2012). Estimating the diets of animals using stable isotopes and a comprehensive Bayesian mixing model. *PLoS ONE*, *7*(1). https://doi.org/10.1371/journal.pone.0028478

IPCC. (2014). *Climate Change 2014: Synthesis Report. Contribution of Working Groups I, II and III to the Fifth Assessment Report of the Intergovernmental Panel on Climate Change*. (Pachauri. R.K. & L. A. Meyer, Eds.) (IPCC). Geneva, Switzerland: IPCC. Retrieved from https://books.google.pt/books?id=o1HLrQEACAAJ

Johannessen, S. C. & Macdonald, R. W. (2016). Geoengineering with seagrasses: is credit due where credit is given? *Environmental Research Letters*, *11*(11). https://doi.org/10.1088/1748-9326/11/11/113001

Kelleway, J. J., Saintilan, N., Macreadie, P. I. & Ralph, P. J. (2016). Sedimentary Factors are Key Predictors of Carbon Storage in SE Australian Saltmarshes. *Ecosystems*, *19*(5), 865–880. https://doi.org/10.1007/s10021-016-9972-3

Kennedy, H., Beggins, J., Duarte, C. M., Fourqurean, J. W., Holmer, M., Marbà, N. & Middelburg, J. J. (2010). Seagrass sediments as a global carbon sink: Isotopic constraints. *Global Biogeochemical Cycles*, *24*(4), n/a-n/a. https://doi.org/10.1029/2010GB003848

Koho, K. A., Nierop, K. G. J., Moodley, L., Middelburg, J. J., Pozzato, L., Soetaert, K., van der Plicht, J. & Reichart, G.-J. (2013). Microbial bioavailability regulates organic matter preservation in marine sediments. *Biogeosciences*, *10*(2), 1131–1141. https://doi.org/10.5194/bg-10-1131-2013

Koschan, A. & Abidi, M. (2008). Color spaces and color distances. In *Digital Color Image Processing* (pp. 125–148). Hoboken, NJ, USA: John Wiley & Sons, Inc. https://doi.org/10.1002/9780470230367.ch6

Kubiszewski, I., Costanza, R., Anderson, S. & Sutton, P. (2017). The future value of ecosystem services: Global scenarios and national implications. *Ecosystem Services*, *26*, 289–301. https://doi.org/10.1016/j.ecoser.2017.05.004

Lahuna, F.-X. (2017). *Sediment deposition in seagrass and salt marsh ecosystems: an approach to quantify ecosystem services in a coastal tidal lagoon*. Master thesis in Oceanography and Marine Environments at University Pierre et Marie Curie.

Lavery, P. S., Mateo, M., Serrano, O. & Rozaimi, M. (2013). Variability in the Carbon Storage of Seagrass Habitats and Its Implications for Global Estimates of Blue Carbon Ecosystem Service. *PLoS ONE*, *8*(9), e73748.

https://doi.org/10.1371/journal.pone.0073748

Li, C.-F., Lin, J., Kulhanek, D. K., Williams, T., Bao, R., Briais, A., Brown, E. A., Chen, Y., Clift, P. D., Colwell, F. S., Dadd, K. A., Ding, W.-W., Hernández-Almeida, I., Huang, X.-L., Hyun, S., Jiang, T., Koppers, A. A. P., Li, Q., Liu, C., et al. (2015). Methods (Vol. 349). https://doi.org/10.14379/iodp.proc.349.102.2015

Machás, R., Santos, R. & Peterson, B. (2006). Elemental and stable isotope composition of Zostera noltii (Horneman) leaves during the early phases of decay in a temperate mesotidal lagoon. *Estuarine, Coastal and Shelf Science*, *66*(1–2), 21–29. https://doi.org/10.1016/j.ecss.2005.07.018

Macreadie, P. I., Allen, K., Kelaher, B. P., Ralph, P. J. & Skilbeck, C. G. (2012). Paleoreconstruction of estuarine sediments reveal human-induced weakening of coastal carbon sinks. *Global Change Biology*, *18*(3), 891–901. https://doi.org/10.1111/j.1365-2486.2011.02582.x

Macreadie, P. I., Ollivier, Q. R., Kelleway, J. J., Serrano, O., Carnell, P. E., Ewers Lewis, C. J., Atwood, T. B., Sanderman, J., Baldock, J., Connolly, R. M., Duarte, C. M., Lavery, P. S., Steven, A. & Lovelock, C. E. (2017). Carbon sequestration by Australian tidal marshes. *Scientific Reports*, *7*, 1–10. https://doi.org/10.1038/srep44071

Maes, J., Egoh, B., Willemen, L., Liquete, C., Vihervaara, P., Schägner, J. P., Grizzetti, B., Drakou, E. G., Notte, A. La, Zulian, G., Bouraoui, F., Luisa Paracchini, M., Braat, L. & Bidoglio, G. (2012). Mapping ecosystem services for policy support and decision making in the European Union. *Ecosystem Services*, *1*(1), 31–39. https://doi.org/10.1016/j.ecoser.2012.06.004

Marbà, N., Arias-Ortiz, A., Masqué, P., Kendrick, G. A., Mazarrasa, I., Bastyan, G. R., Garcia-Orellana, J. & Duarte, C. M. (2015). Impact of seagrass loss and subsequent revegetation on carbon sequestration and stocks. *Journal of Ecology*, *103*(2), 296–302. https://doi.org/10.1111/1365-2745.12370

Mateo, M. A., Cebrián, J., Dunton, K. & Mutchler, T. (2006). Carbon Flux in Seagrass Ecosystems. In *Seagrasses: Biology, Ecology and Conservation* (pp. 159–192). Berlin/Heidelberg: Springer-Verlag. https://doi.org/10.1007/1-4020-2983-7_7

Mateo, M. A., Romero, J., Pérez, M., Littler, M. M. & Littler, D. S. (1997). Dynamics of

Millenary Organic Deposits Resulting from the Growth of the Mediterranean SeagrassPosidonia oceanica. *Estuarine, Coastal and Shelf Science*, *44*(1), 103–110. https://doi.org/10.1006/ecss.1996.0116

Mateo, M. A., Sánchez-Lizaso, J. L. & Romero, J. (2003). Posidonia oceanica "banquettes": a preliminary assessment of the relevance for meadow carbon and nutrients budget. *Estuarine, Coastal and Shelf Science*, *56*(1), 85–90. https://doi.org/10.1016/S0272-7714(02)00123-3

McLeod, E., Chmura, G. L., Bouillon, S., Salm, R., Björk, M., Duarte, C. M., Lovelock, C. E., Schlesinger, W. H. & Silliman, B. R. (2011). A blueprint for blue carbon: Toward an improved understanding of the role of vegetated coastal habitats in sequestering CO2. *Frontiers in Ecology and the Environment*, *9*(10), 552–560. https://doi.org/10.1890/110004

Millennium Ecosystem Assessment. (2005). *Ecosystems and Human Well-being: Synthesis*. Island Press. Retrieved from https://books.google.pt/books?id=2nhzQgAACAAJ

Miyajima, T., Hori, M., Hamaguchi, M., Shimabukuro, H., Adachi, H., Yamano, H. & Nakaoka, M. (2015). Geographic variability in organic carbon stock and accumulation rate in sediments of East and Southeast Asian seagrass meadows. *Global Biogeochemical Cycles*, *29*(4), 397–415. https://doi.org/10.1002/2014GB004979

Nellemann, C., Corcoran, E., Duarte, C. M., Valdés, L., De Young, C., Fonseca, L. & Grimsditch, G. (Eds.). (2009). *Blue carbon: A Rapid Response Assessment*. *United Nations Environment Programme*. GRID-Arendal. Retrieved from http://www.grida.no

Núñez, N. D. (2015). *Comparing Zostera and Spartina environments in relation to carbon burial: a sedimentary and geochemical approach from Ria Formosa*. Master thesis in Marine Biology in University of Algarve.

Parnell, A. (2016). simmr: A Stable Isotope Mixing Model. Retrieved from https://cran.r-project.org/package=simmr

Parnell, A. C., Phillips, D. L., Bearhop, S., Semmens, B. X., Ward, E. J., Moore, J. W., Jackson, A. L., Grey, J., Kelly, D. J. & Inger, R. (2013). Bayesian stable isotope

mixing models. *Environmetrics*, *24*(6), 387–399. https://doi.org/10.1002/env.2221

Phillips, D. L. & Gregg, J. W. (2003). Source partitioning using stable isotopes: Coping with too many sources. *Oecologia*, *136*(2), 261–269. https://doi.org/10.1007/s00442-003-1218-3

Phillips, D. L., Inger, R., Bearhop, S., Jackson, A. L., Moore, J. W., Parnell, A. C., Semmens, B. X. & Ward, E. J. (2014). Best practices for use of stable isotope mixing models in. *Canadian Journal of Zoology*, *835*(August), 823–835. https://doi.org/10.1139/cjz-2014-0127

Ricart, A. M., York, P. H., Rasheed, M. A., Pérez, M., Romero, J., Bryant, C. V. & Macreadie, P. I. (2015). Variability of sedimentary organic carbon in patchy seagrass landscapes. *Marine Pollution Bulletin*, *100*(1), 476–482. https://doi.org/10.1016/j.marpolbul.2015.09.032

Röhr, M. E., Boström, C., Canal-Vergés, P. & Holmer, M. (2016). Blue carbon stocks in Baltic Sea eelgrass (*Zostera marina*) meadows. *Biogeosciences Discussions*, (April), 1–38. https://doi.org/10.5194/bg-2016-131

Schneider, C. A., Rasband, W. S. & Eliceiri, K. W. (2012). NIH Image to ImageJ: 25 years of image analysis. *Nature Methods*, *9*(7), 671–675. https://doi.org/10.1038/nmeth.2089

Serrano, O., Lavery, P., Masque, P., Inostroza, K., Bongiovanni, J. & Duarte, C. (2016a). Seagrass sediments reveal the long-term deterioration of an estuarine ecosystem. *Global Change Biology*, *22*(4), 1523–1531. https://doi.org/10.1111/gcb.13195

Serrano, O., Ricart, A. M., Lavery, P. S., Mateo, M. A., Arias-Ortiz, A., Masque, P., Rozaimi, M., Steven, A. & Duarte, C. M. (2016b). Key biogeochemical factors affecting soil carbon storage in Posidonia meadows. *Biogeosciences*, *13*(15), 4581–4594. https://doi.org/10.5194/bg-13-4581-2016

Shi, J. Z. (2009). Review of The Dynamics of Coastal Models by Clifford J. Hearn 2008. *Journal of Coastal Research*, *25*, 1064–1065. https://doi.org/10.2112/JCOASTRES-D-09-00023.1

Sutton, P. C., Anderson, S. J., Costanza, R. & Kubiszewski, I. (2016). The ecological economics of land degradation: Impacts on ecosystem service values. *Ecological Economics*, *129*(October 2017), 182–192.

https://doi.org/10.1016/j.ecolecon.2016.06.016

Trumper, K., Bertzky, M., Dickson, B., van Der Heijden, G., Jenkins, M. & Manning, P. (2009). *The Natural Fix? The role of ecosystems in climate mitigation. A UNEP rapid response assessment. Director*. https://doi.org/978-82-7701-057-1

Tyler-Walters, H. (2005). Zostera (Zosterella) noltei Dwarf eelgrass. In T.-W. H. & H. K. (Eds.), *Marine Life Information Network: Biology and Sensitivity Key Information Reviews, [on-line]*. Plymouth: Marine Biological Association of the United Kingdom. Retrieved from http://www.marlin.ac.uk/species/detail/1409

Watanabe, K. & Kuwae, T. (2015). How organic carbon derived from multiple sources contributes to carbon sequestration processes in a shallow coastal system? *Global Change Biology*, *21*(7), 2612–2623. https://doi.org/10.1111/gcb.12924

Wills, S. A., Burras, C. L. & Sandor, J. A. (2007). Prediction of Soil Organic Carbon Content Using Field and Laboratory Measurements of Soil Color. *Soil Science Society of America Journal*, *71*(2), 380. https://doi.org/10.2136/sssaj2005.0384

Zelenak, M. (1995). *Relationship between Munsell color value and organic carbon content in Montana soils*. *Montana State University*. Montana State University. Retrieved from https://www.tandfonline.com/doi/full/10.1080/00103627909366981

ANNEXES

ANNEX 1 – Sample exclusion for SIMM

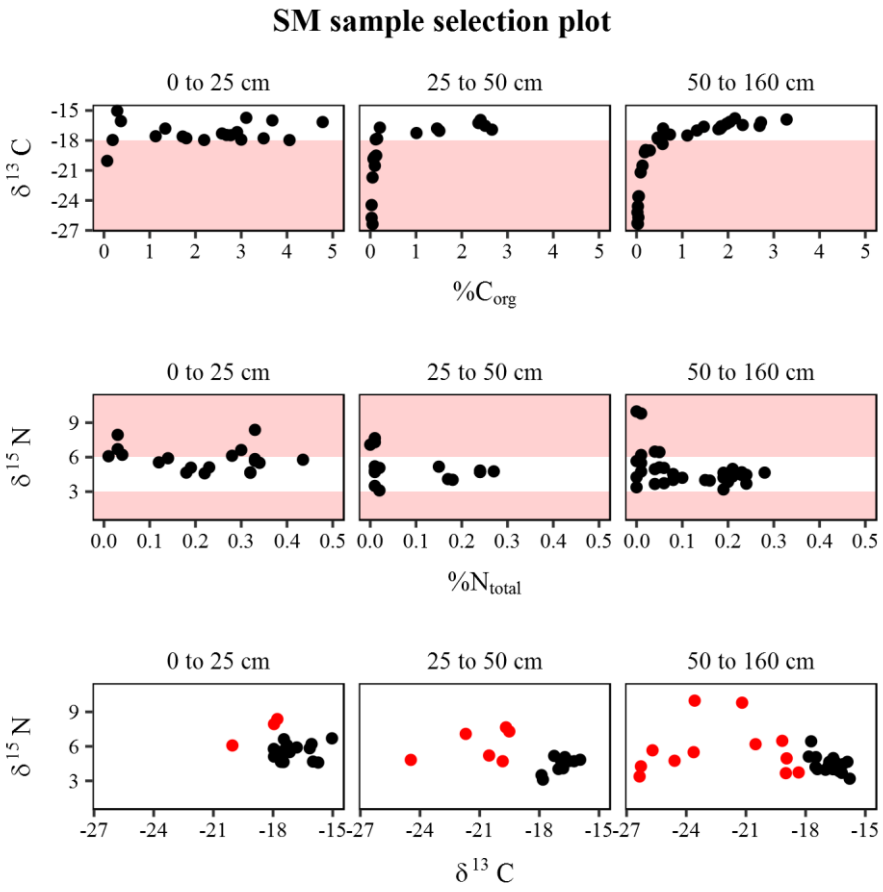

Figure 1.1 - Scatterplots of isotopic signatures vs elemental contents and δ15N vs $\delta 13C_{org}$ for SM samples. Low C_{org} contents were associated with a lower $\delta 13C_{org}$, suggesting that degradation of organic matter in those samples affected $\delta^{13}C_{org}$; low N_{total} was related to an increase in the variance of $\delta^{15}N$, once again suggesting possible effects from organic matter degradation. Samples with largest alterations (inside red area in top 2 rows) were excluded (marked in red in bottom row)

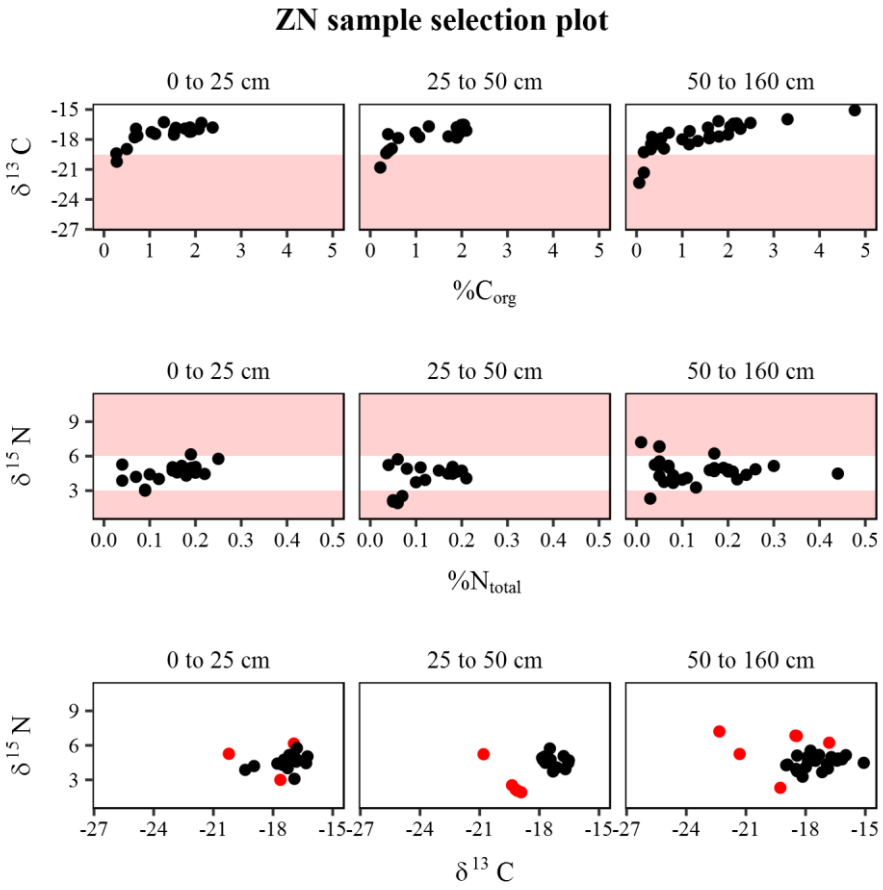

Figure 1.2 - Scatterplots of isotopic signatures vs elemental contents and δ15N vs $\delta^{13}C_{org}$ for ZN samples. Low C_{org} contents were associated with a lower $\delta^{13}C_{org}$, suggesting that degradation of organic matter in those samples affected $\delta^{13}C_{org}$; low N_{total} was related to an increase in the variance of $\delta^{15}N$, once again suggesting possible effects from organic matter degradation. Samples with largest alterations (inside red area in top 2 rows) were excluded (marked in red in bottom row).

ANNEX 2 – Core profile pictures vs C_{org} content

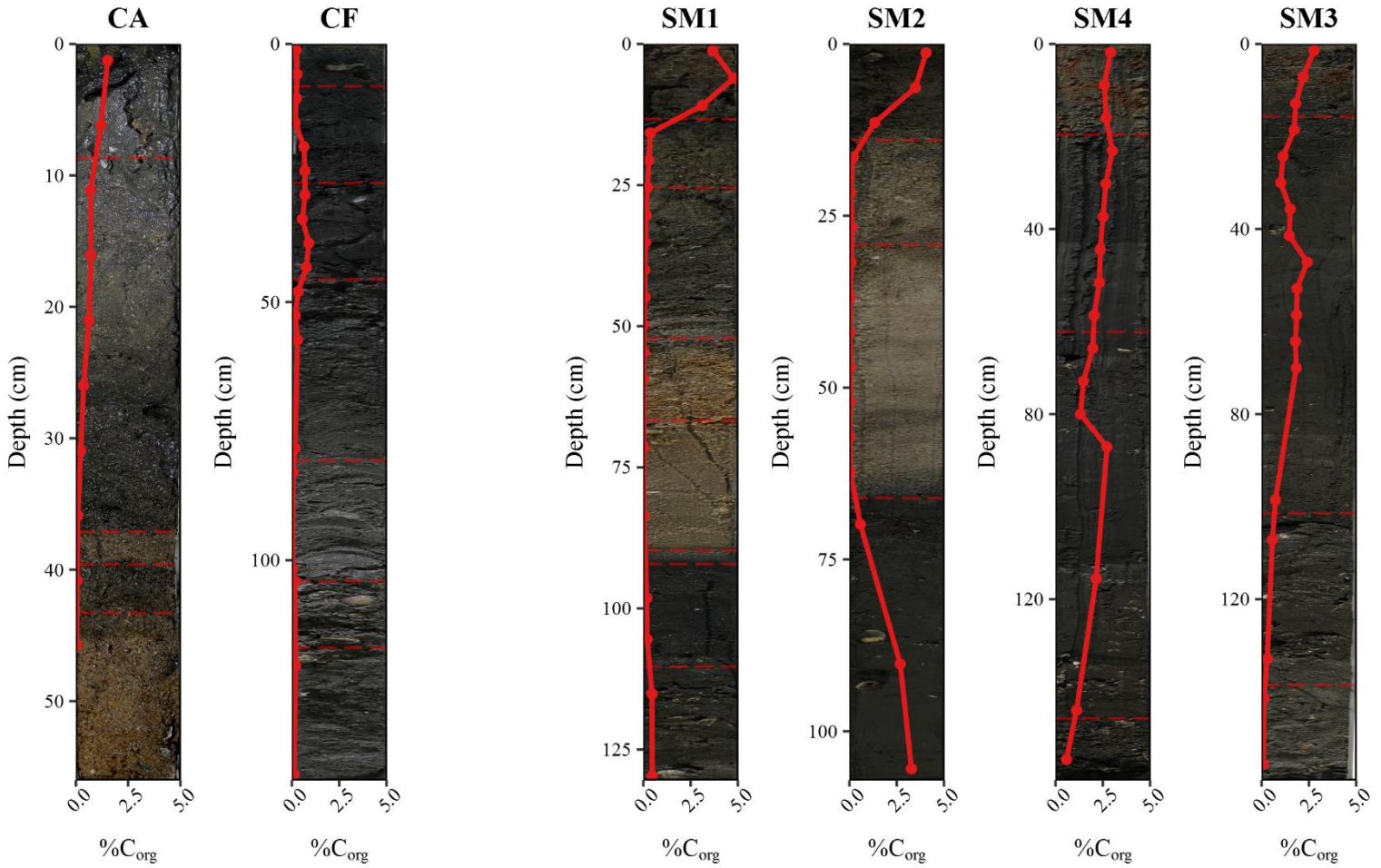

Figure 2.1 - $\%C_{org}$ over depth in CA, CF and SM cores, plotted over the photographed core profile. Due to the processing required to obtain the profiles, photography's depths might have alignment errors. Horizons that were visually described (see Figure 3.5) are plotted as red horizontal lines to help interpret the profile. Note: both X and Y axis are on different scales

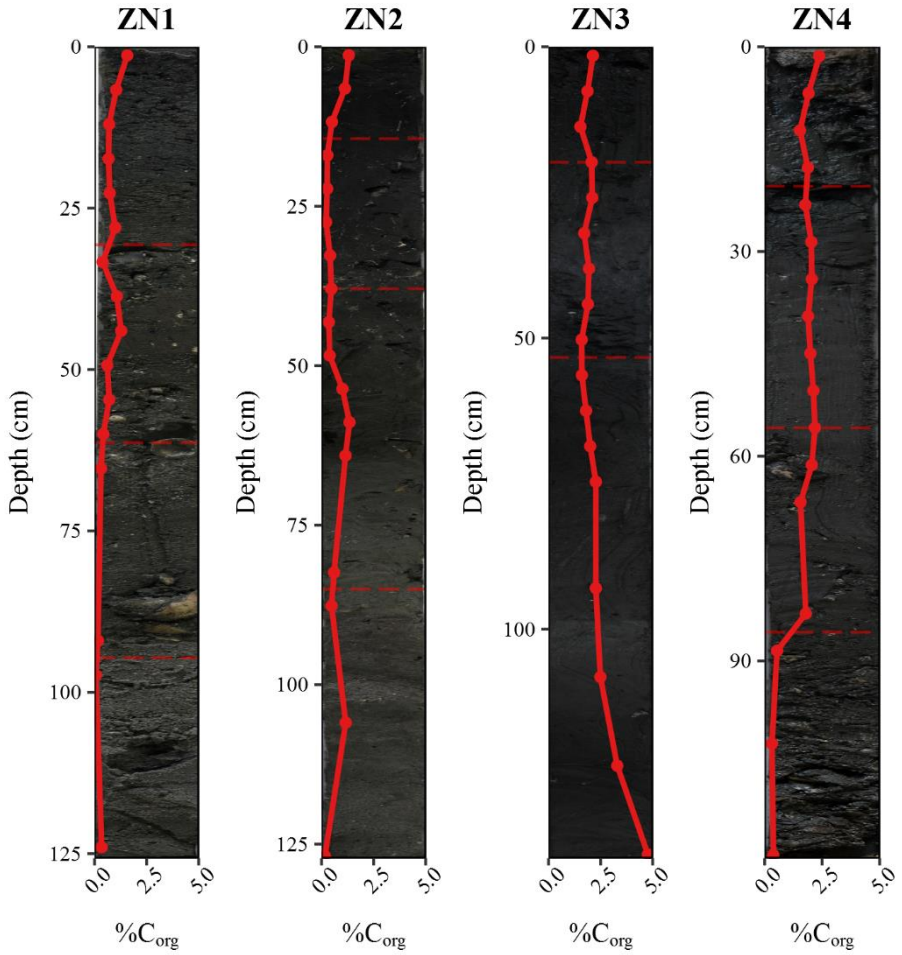

Figure 2.2 - %C_{org} over depth in ZN cores, plotted over the photographed core profile. Due to the processing required to obtain the profiles, photography's depths might have alignment errors. Horizons that were visually described (see Figure 3.5) are plotted as red horizontal lines to help interpret the profile. Note: both X and Y axis are on different scales